

INTEGRINS IN THE OPTIC NERVE HEAD: POTENTIAL ROLES IN GLAUCOMATOUS OPTIC NEUROPATHY (AN AMERICAN OPHTHALMOLOGICAL SOCIETY THESIS)

BY John C. Morrison MD

ABSTRACT

Purpose: To demonstrate that specific distributions of integrin-based focal mechanoreceptors exist in primate optic nerve heads, suitable for translating stress and strain into the cellular responses of glaucomatous optic neuropathy.

Methods: Normal human (N = 20) and rhesus monkey (N = 14) optic nerve heads and 32 glaucomatous optic nerve heads were processed for immunohistochemistry to determine the structural distribution of integrin subunits $\alpha 1$, $\alpha 2$, $\alpha 3$, $\alpha 4$, $\alpha 5$, $\alpha 6$, αv , $\beta 1$, $\beta 2$, $\beta 3$, and $\beta 4$. Labeling patterns in glaucoma specimens were compared with those of normal eyes.

Results: In all specimens, cells within collagenous laminar beams and sclera failed to label with any integrin antibodies. In normal eyes, $\alpha 2$, $\alpha 3$, $\alpha 6$, $\beta 1$, and $\beta 4$ antibodies localized to astrocytes along the margins of laminar beams and within glial columns. $\alpha 3$, $\alpha 5$, $\alpha 6$, αv , $\beta 1$, and $\beta 4$ labeled vascular endothelial cells. In severely damaged glaucoma specimens, cells anterior to the compressed lamina cribrosa displayed persistent label for $\alpha 2$, $\alpha 3$, $\beta 1$, and $\beta 4$, whereas label for $\alpha 4$ increased and $\alpha 6$ was decreased.

Conclusions: Integrins $\alpha 2\beta 1$, $\alpha 3\beta 1$, $\alpha 6\beta 1$, and $\alpha 6\beta 4$ may provide attachment for astrocytes to basement membranes via laminin, providing opportunities to sense changes in stress and strain within and anterior to the lamina cribrosa. Vascular endothelial cell stress may be mediated by integrins $\alpha 3\beta 1$, $\alpha 6\beta 1$, and $\alpha 6\beta 4$, along with $\alpha 5\beta 1$ and $\alpha v\beta 1$. In advanced damage, reduced $\alpha 6$ label and variable label for $\beta 4$ anterior to the lamina cribrosa suggests astrocyte migration. Increased label for $\alpha 4$ subunits suggests activation of microglia.

Trans Am Ophthalmol Soc 2006;104:453-477

INTRODUCTION

Glaucoma is an irreversible, blinding disease that presently affects over 2.22 million people in the United States and is expected to affect 3.36 million by the year 2020.¹ Throughout the world, it is now considered the second most prevalent cause of blindness.² Glaucoma patients suffer inexorable, progressive loss of vision that, in the majority of cases, is painless and without symptoms until late in the disease. Currently, the exact cellular mechanisms of vision loss are unknown, despite intense investigation.

Clinically, recognition of several risk factors provides valuable information for diagnosis in glaucoma. These include intraocular pressure (IOP), age, family history, clinical appearance of the optic nerve, race, and potentially, vascular disease.³⁻⁶ Of these, IOP remains the most prominent, and treatment of IOP is the mainstay of nearly all current glaucoma therapy.

In recent years, several large clinical trials have shown that IOP reduction with either medicines or surgery can reduce the development and progression of vision loss in patients with advanced glaucoma,⁷ normal pressure glaucoma,⁸ and in patients with ocular hypertension but no apparent glaucomatous optic nerve damage.⁹ However, in all of these studies there were patients who continued to suffer progressive vision loss, despite apparently adequate pressure control. This suggests that, in some patients, the extent of pressure lowering may not have been sufficient to provide complete protection, whereas in others, factors unrelated to IOP may be active. It is also possible that yet other factors, currently poorly understood, can interface with IOP to enhance glaucomatous optic nerve damage. It remains possible that manipulation of such factors may lead to new treatments that can augment conventional pressure-lowering therapy and more effectively protect vision in glaucoma patients. Better understanding of the cellular mechanisms by which IOP produces glaucomatous optic nerve damage is essential for revealing these adjunctive treatments.

In recent years, new concepts of understanding the optic nerve head as a biomechanical structure have emerged.¹⁰⁻¹² In this paradigm, stress and strain due to changes in IOP will be distributed within the optic nerve head according to the architecture and composition of its load-bearing connective tissue structures. These structures, largely made up of the extracellular matrix (ECM), are most likely the lamina cribrosa and peripapillary sclera. Through mechanisms that are currently unknown, these forces may be ultimately translated into cellular responses that constitute glaucomatous optic nerve damage. An inherent feature of this paradigm is the existence of specialized molecules within the optic nerve head that are capable of sensing connective tissue forces and transmitting them into cellular responses.

A major mechanism by which cells communicate with their environment is through integrin-mediated cell adhesion.^{13,14} Integrins are membrane-spanning proteins that bind to ligands in the ECM and interact intracellularly with the cytoskeleton. This binding, particularly when augmented by applied force, as may occur from ECM stress, activates the intracellular domain of the molecule and focal adhesions, molecular complexes composed of over 50 proteins that link the integrins to the actin cytoskeleton. This activation can result in changes to a wide variety of cellular functions, including cell motility, shape change, and survival and proliferation.¹⁵

The central hypothesis of this thesis is that integrins are present throughout the primate optic nerve head in distributions that would allow cells within specific structures to respond to stress and strain. The most likely of these structures are anticipated to be the load-

From the Oregon Health and Science University, Casey Eye Institute, Portland, Oregon. Supported by grants EY10145 and EY16866 from the National Institutes of Health and unrestricted funds from Research to Prevent Blindness. All work has been performed at the Casey Eye Institute. The author discloses no financial interests in this article.

bearing lamina cribrosa and peripapillary sclera, in addition to arterioles and capillaries of the entire optic nerve head.

Based upon the known distributions of ECM ligands within the optic nerve head, it is anticipated that $\alpha 1$, $\alpha 2$, and $\beta 1$ integrin subunits will be present in cells within the collagen-containing laminar beams and peripapillary sclera. The presence of laminin within basement membranes would further suggest that $\alpha 1$, $\alpha 2$, $\alpha 3$, $\alpha 5$, $\alpha 6$, $\beta 1$, and $\beta 4$ would be found surrounding laminar beams and within blood vessels, primarily associated with astrocytes and vascular endothelium. This is further supported by described associations of specific integrin subtypes within the central nervous system.

The first step in evaluating this hypothesis involves determining if integrins are present in the optic nerve head and where they are located. To accomplish this, normal human and nonhuman primate optic nerve heads and glaucomatous human optic nerve heads were analyzed immunohistochemically, using a battery of antibodies specific for different integrin subunits known to bind to many components of the ECM. The presence and distribution patterns of these subunits are compared to those of their respective ECM ligands to determine the most likely integrin heterodimers in normal tissues, and their cells of origin. Further comparisons of these patterns with those of eyes with glaucomatous optic nerve damage were then performed to provide clues to their possible roles in glaucomatous optic neuropathy.

CLINICAL CHARACTERISTICS OF GLAUCOMA

Clinically, glaucoma is diagnosed by “cupping” of the optic nerve head and a characteristic pattern of visual field loss. Cupping, usually most pronounced in the superior and inferior regions, results from the loss of retinal ganglion cell (RGC) axons and the posterior bowing and remodeling of the lamina cribrosa.^{16,17} Clinicopathologic studies of glaucomatous eyes document that axons in the superior and inferior optic nerve atrophy first, producing an “hour-glass” injury pattern and glaucomatous visual field loss.¹⁸ The most characteristic visual field defect is the arcuate scotoma, which can arch above or below central fixation without crossing the horizontal midline, following the pathways of the RGC nerve fiber bundles as they converge on the superior and inferior poles of the optic nerve head.^{19,20}

At present, only the structure of the optic nerve head has been shown to correlate with this pattern of injury. In humans, the laminar beams of the superior and inferior optic nerve head are less dense, with larger pores between them, as compared to those in the nasal and temporal regions.²¹ This correlation of the lamina cribrosa anatomy with the increased susceptibility of the superior and inferior optic disc suggests strongly that the optic nerve head is an initial site of damage and vision loss in glaucoma. Understanding the structure of the optic nerve head and the cellular alterations produced by changes in IOP are likely to help us understand mechanisms of glaucomatous optic nerve damage.

STRUCTURE OF THE PRIMATE OPTIC NERVE HEAD

The primate optic nerve head can be considered in four levels.^{22,23} From anterior to posterior, these layers are (1) the nerve fiber layer, (2) the lamina choroidalis, (3) the lamina cribrosa, and (4) the retrobulbar optic nerve.

Unmyelinated RGC axons in the nerve fiber layer of the retina converge on the optic nerve head. As they progress into the optic nerve head, axons become increasingly segregated into bundles and turn posteriorly to begin their exit from the globe. This occurs at the level of the choroid, and the glial support tissues are here termed the lamina choroidalis. This is composed primarily of stellate-shaped astrocyte cell bodies that are ordered into columns (glial columns) parallel to the axon bundles and interconnected by their processes in a basket-like arrangement. Extensions from these processes also enter the axon bundles, interdigitating and providing intimate contact with the axons (Figure 1A).

As the axon bundles approach the sclera, increasing amounts of ECM materials appear between them, in association with the glial columns. At the level of the sclera, the ECM forms the lamina cribrosa, or lamina scleralis. The lamina cribrosa consists of several connective tissue plates that extend across the optic nerve head from the edges of the scleral opening at the back of the eye. Each plate is perforated, with the pores lining up with those of adjacent plates to allow the nerve fiber bundles to pass through the sclera and out the eye. The plates themselves, or beams, are lined by astrocytes resting on basement membranes, effectively separating the ECM from the nerve fiber bundles (Figure 1B). The composition of the lamina cribrosa will be described in the following section. As in the lamina choroidalis, astrocyte processes extend into the axon bundles. The retrobulbar, or intraorbital, optic nerve begins at the posterior border of the lamina cribrosa, where the axons become myelinated and their bundles are separated by collagenous septa.

Early descriptions of the vasculature of the primate optic nerve head relied upon detailed observations of serial histologic sections.²⁴ These resulted in the appreciation that blood supply to the optic nerve head is essentially a centripetal system, with derivation of capillary beds from the branches from the posterior ciliary arteries. Venous blood drains from the capillary bed at all levels of the optic nerve head into the central retinal vein.

In later years, the development of methylmethacrylate polymer systems allowed the microinjection of entire vascular beds. When combined with tissue digestion using heated sodium hydroxide, this technique resulted in highly detailed castings of arterioles, capillaries, and venules that could be examined in detail by scanning electron microscopy, due the high stability of the hardened plastic. Later modifications of this formula resulted in reduced viscosity of the injection medium, allowing injection at relatively physiologic pressures and improving filling of vascular systems, even in postmortem specimens.²⁵⁻²⁷

These detailed microvascular injection methods confirmed the initial observations of Hayreh, demonstrating the overriding importance of the posterior ciliary artery system.^{24, 27} The only exception to this is within the nerve fiber layer, where capillaries arise from the central retinal artery. Within the laminar and retrolaminar regions of the optic nerve head, arteriole branches from the posterior ciliary arteries form the circle of Zinn-Haller, which supplies the capillary beds of the lamina choroidalis and lamina

cribrosa. Anteriorly, the capillaries of the choroidal lamina are ensheathed by astrocytes within the glial columns. More posteriorly, capillaries are encased within the laminar beams of the lamina cribrosa, and in the septa of the postlaminar, or retrobulbar optic nerve (Figure 1B). Anatomically, a continuous capillary bed exists through all layers of the optic nerve head, although it is uncertain if connections between the different regions are physiologic and functional.

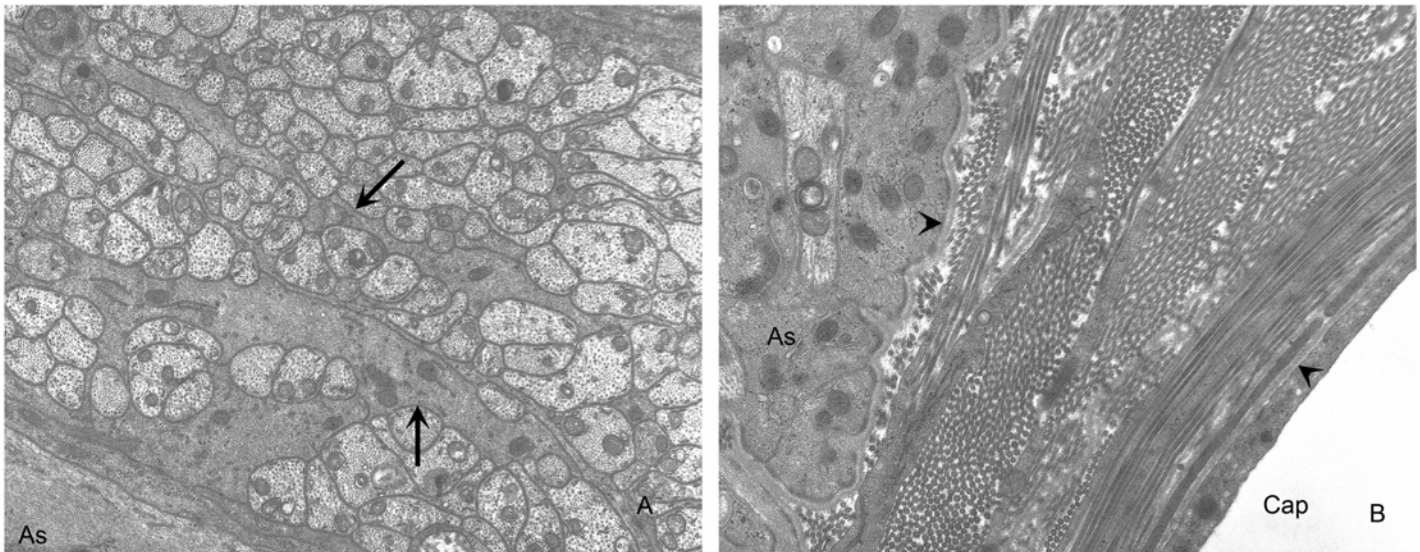


FIGURE 1

Ultrastructure of the optic nerve head. A, Astrocyte glial processes (arrows) demonstrate intimate relationships to optic nerve axons (cut in cross section). B, Within laminar beam, fibrillar collagen (cut in cross section and longitudinally) is interposed between capillary and astrocytes lining the beam itself. Note basement membranes (arrowheads) of capillary endothelial cells and astrocytes. As, astrocytes; Cap, capillary. (Magnification $\times 40,000$)

EXTRACELLULAR MATRIX OF THE PRIMATE OPTIC NERVE HEAD

Because of the potential importance of the optic nerve head as an initial site of glaucomatous optic nerve damage, researchers have long been interested in its composition as well as its structure. This is primarily reflected in the ECM of the sclera and the connective tissues of the lamina cribrosa and retrobulbar optic nerve septae.

In all tissues, the ECM provides structural properties that range from tensile strength to resiliency, cell attachment, organization, and barrier functions. In the optic nerve head, the physical behavior of the ECM, which depends heavily on the composition of its structural elements, will influence the behavior of this tissue to changes in IOP and is likely to affect the development of glaucomatous optic nerve damage.

Early descriptions of the histology of the optic nerve head documented that it consisted of fibrillar collagen within the laminar beams with interspersed elastic tissue and basement membranes.^{22,23} Subsequent evaluations using immunohistochemical methods at both the light and transmission electron microscopic levels have provided many of the specifics of this composition.²⁸⁻³³ These techniques have confirmed that the major ECM proteins of the optic nerve head consist of collagens 1, 3, 5, and 6, along with elastin in the peripapillary sclera, the cores of laminar beams, and retrobulbar optic nerve septae. In addition to this, the basement membrane components laminin and collagen 4 were identified along the margins of the laminar beams in association with astrocytes, and within the beams, in association with capillary vascular endothelium.³³ Similar labeling patterns were also seen extending laterally from the lamina cribrosa into the peripapillary sclera (the insertion zone), and posteriorly over the optic nerve septa, perineurium, and optic nerve sheath of the retrobulbar optic nerve. Similar findings have since been reported in the normal rodent optic nerve head.³⁴ This, along with documentation that the rat optic nerve head microvascular anatomy has many features in common with that of the primate eye,³⁵ strongly supports the validity of observations obtained from chronically elevated IOP in this animal model.

A subsequent study identified the presence and distribution of chondroitin and dermatan sulfate-containing proteoglycans (PG) in the primate optic nerve head.³⁶ Proteoglycans, major components of the ECM, are a large group of proteins that have attached carbohydrate side chains, or glycosaminoglycans. Because glycosaminoglycans adhere to many other macromolecules through charge interactions, they are very important to the interrelationships between the above-described ECM components and can influence the physical behavior of the ECM.

These results confirmed that chondroitin and dermatan sulfate-containing PG are localized to regions previously shown to contain large amounts of fibrillar collagen. However, preincubation of tissues with enzymes that expose primarily chondroitin sulfate attachment sites revealed that some PG are more restricted to the lamina cribrosa and peripapillary sclera, tissues that are load-bearing structures of the optic nerve head and more likely to be exposed to IOP. The retrobulbar optic nerve septae, sheath, and perineurium

did not label with this preparation. This observation constitutes an early suggestion that some ECM components have a specific regional presence and contribute unique properties to the lamina cribrosa and peripapillary sclera. Similar observations on the distribution of aggrecan, a specific chondroitin sulfate PG, and other ECM components, as well as integrins, provide further support for this possibility, and will be presented later.

PATHOLOGY OF GLAUCOMATOUS OPTIC NERVE DAMAGE AND THE SITE OF INJURY

Our current understanding of the pathology of glaucomatous optic nerve damage is derived from the study of human specimens, in conjunction with specific analysis of animal eyes with experimental elevations of IOP. Using trypsin digest preparations of normal and glaucomatous human optic nerve heads to reveal the more resistant collagenous lamina cribrosa, Quigley and colleagues^{16,18} confirmed the predilection for glaucoma to produce cupping of the superior and inferior poles of the nerve head. They also demonstrated that this cupping resulted from posterior bowing of the lamina cribrosa, combined with collapse and compression of the laminar sheets and loss of neural tissue. Whereas it was also suggested that loss of astrocytes, the supportive cells of the optic nerve head, was in some way responsible for the loss of axons, specific study of astrocyte numbers did not support this possibility.¹⁸

Ultrastructural studies of human glaucoma specimens also demonstrated an accumulation of organelles in axons at the level of the lamina cribrosa.¹⁶ In addition, experimental studies in monkeys indicate that obstructed axonal transport is localized to this region.³⁷⁻⁴¹ Obstruction of retrograde transport of BDNF and its trkB receptor within the optic nerve head has also been demonstrated in rats, and axon transport blockade at the level of the lamina cribrosa is proposed to play a critical role in producing RGC damage in glaucoma.⁴³

CELL BIOLOGY OF OPTIC NERVE HEAD CHANGES IN GLAUCOMA

Over the past two decades, considerable knowledge has accumulated on the cell biology of glaucomatous optic nerve damage, suggesting that the injury is an active biological process, rather than simple, passive compromise of axons. These data have emerged from a series of studies ranging from the evaluation of human specimens with glaucomatous optic nerve damage, primate and rodent models of experimentally elevated IOP, and organ and cell culture of primate optic nerve heads, combined with experimental manipulation of environmental factors, such as hydrostatic pressure.

In 1990, two papers were published describing ECM alterations in glaucoma⁴⁴ and in nonhuman primate eyes with experimentally elevated IOP.⁴⁵ In glaucomatous optic nerve heads, Hernandez and associates⁴⁴ found increased label of collagen type 6, and extension of collagen type 4 and other basement membrane macromolecules in between the laminar beams, into regions occupied by axon bundles in normal eyes. This same group later analyzed mRNA production for collagen type 4 in eyes with primary open-angle glaucoma and found evidence for increased mRNA production within astrocytes in the prelaminar region of the optic nerve head, as well as within the compressed lamina cribrosa.⁴⁶ This confirmed the increased production of ECM in glaucoma and supported the concept that at least some of this production resided within astrocytes.

Morrison and colleagues⁴⁵ showed that chronic elevation of IOP in monkey eyes also produced increased label for collagen types 1, 3, and 4 within the pores of the laminar beams. Interestingly, there was no evidence of ECM deposition within the laminar beam pores in eyes with optic nerve transection. These results, combined with the data of Hernandez,⁴⁴ indicate that at least some of these ECM changes are unique to the glaucomatous process, and related to elevated IOP, rather than a simple response to loss of RGC axons and nerve fiber bundles.

Similar ECM alterations were later documented in a model of chronic IOP elevation and optic nerve damage in rats.^{47,48} In addition, Johnson and colleagues,⁴⁹ using this same model, studied the chronology of several optic nerve head responses following experimental induction of elevated IOP. They found that early changes occurring first within the optic nerve head included loss of gap junctional connexin 43 and increased proliferation of astrocytes, along with a depletion of optic nerve head neurotrophin labeling and the spread of immunolabeling for collagen type 6.

Hernandez' group has also studied the behavior of tenascin C in human glaucomatous optic nerve heads. They found that mRNA for this large glycoprotein, which has been linked to tissue remodeling in wound healing and tumorigenesis, was upregulated in astrocytes, both in the prelaminar and laminar regions.⁵⁰

As noted above, loss of structural optic nerve head organization is an important feature of glaucomatous optic neuropathy. This process, also called remodeling, involves cellular migration, which also depends upon the degradation of connective tissues. Degradation of the ECM is carried out in part by matrix metalloproteinases (MMPs) and tissue inhibitors of MMPs (TIMPs). Based on the extent of tissue remodeling, MMPs would also be expected to change during glaucoma. In fact, Hernandez' group has demonstrated increased immunoreactivity for specific MMPs associated with astrocytes in human glaucomatous optic nerve heads.⁵¹ They later corroborated this finding in monkeys with experimental IOP elevation⁵² but did not find this in eyes with experimental optic nerve transection. This supports the earlier observation that ECM deposition in experimental glaucoma is specific to elevated IOP.⁴⁵

Additional studies concentrating on astrocytes in optic nerve heads from glaucomatous eyes have demonstrated other specific responses, including increased production of GFAP and alterations in astrocyte cell shape, as well as their appearance within the optic nerve bundles, rather than in association with laminar beams.^{50,53} Both observations strongly suggest that astrocytes of the optic nerve head may lose their normal attachments to the ECM and migrate in glaucoma.

A later study, using microarray technology of astrocytes cultured from normal and glaucomatous optic nerve heads, further supports the concept that glaucomatous optic nerve damage involves a wide range of cellular responses.⁵⁴ This group found

differential expression of 150 genes, representing several cell processes, including signal transduction, cell adhesion, and synthesis, and ECM production and degradation. In a similar approach, a microarray analysis of cultured human optic nerve head astrocytes compared to those grown under increased hydrostatic pressure revealed specific increases in genes coding for signal transduction and those involved in transcription regulation, as well as genes associated with lipid metabolism.⁵⁵

Johnson and colleagues, working with a rat model of chronically elevated IOP, have used spotted microarray technology to determine gene responses in optic nerve heads of eyes with chronic and severe ongoing pressure-induced optic nerve damage and confirmed many of the above findings. (Johnson E, Association for Research in Vision and Ophthalmology, 2005, Abstract 1243) They demonstrated significant up-regulation of gene families including cell proliferation, transcription, translation, and protein transport. Specific changes were found in genes related to cellular adhesion and communication, including upregulation of several ECM components (collagens 1, 3, 4, and 6) and matrix metalloproteinases. The ECM proteins periostin and tenascin C were among the most upregulated mRNAs. Of particular relevance to this thesis, they also found differential regulation of many proteins that participate in integrin-mediated cell adhesion.

All of these studies support the concept that cells of the optic nerve head, including astrocytes, demonstrate a variety of cellular responses in the glaucomatous process, and many can be triggered by elevated IOP. As will be discussed below, many of these responses are represented in the repertoire of integrin functions. The broad agreement among findings from human glaucoma specimens, and rat and monkey models, as well as organ and tissue culture studies, argues strongly for the universal nature of many of these observations.

MECHANISMS OF GLAUCOMATOUS OPTIC NERVE DAMAGE

The relationship of the pattern of optic nerve injury and visual field loss in glaucoma to the anatomy of the lamina cribrosa suggests that glaucomatous optic nerve damage is heavily influenced by the connective tissue structure of the optic nerve head. Initial descriptions of these relationships were accompanied by speculation that damage to axons from elevated IOP resulted from posterior movement and scissoring of the thinner, weaker laminar beams of the superior and inferior lamina cribrosa against the optic nerve bundles.²¹ This has been called the mechanical hypothesis. Alternatively, since capillaries lie within the laminar beams, this pattern could also result in regional alterations in blood flow due to collapse of less well protected vessels in the thinner beams.⁵⁶ This is known as the vascular hypothesis.

To date, experimental support for both the mechanical and vascular hypotheses has been elusive. The cellular events that connect the regional pattern of glaucomatous optic nerve damage with the structural anatomy of the optic nerve head are still unknown.

In recent years, another concept has been proposed that encompasses both the unique anatomic structure of the lamina cribrosa and the known cell biology of glaucomatous optic neuropathy. Using engineering principles, this theory considers the optic nerve head as a biomechanical structure.¹⁰⁻¹² It is proposed that the forces resulting in glaucomatous optic nerve damage emanate from alterations in stress generated by changes in IOP in the peripapillary sclera and the other connective tissues of the optic nerve head, especially the lamina cribrosa. The intimate anatomic relationships of astrocytes to the laminar beams and the axon bundles provide a potential pathway by which these stresses can then be translated into nerve injury.

Using a finite element modeling approach, Bellezza and colleagues¹⁰ have demonstrated that specific configurations of the optic nerve head, such as a thinner peripapillary sclera and a more elliptical and larger scleral canal, will all increase the stress (force per cross-sectional area) within the optic nerve head for any given level of IOP. From this, they have calculated that the IOP-related stress at the scleral opening and within the lamina cribrosa will be 73 and 122 times IOP, respectively. Thus, stress within the optic nerve head is considerable, even in eyes with normal IOP. In addition, other anatomic characteristics, such as a larger scleral canal or weak laminar beams, could also be significant contributors to glaucomatous optic nerve damage.

From these considerations, this group has proposed that the pattern of glaucomatous injury is governed by the stress (force per cross-sectional area) and strain (local deformation) that exists within the optic nerve head. They further propose that these forces are heavily influenced by the three-dimensional geometry and material properties of the load-bearing tissues of the optic nerve head, notably, the peripapillary sclera and lamina cribrosa.

In support of this theory, Burgoyne and associates¹² have used high-resolution, three-dimensional reconstructions to study the connective tissues of the optic nerve head in monkey eyes with elevated IOP. In eyes with early evidence of glaucomatous injury, such as the onset of fixed (permanent) posterior deformation of the optic nerve head surface or increased posterior movement of the optic nerve head following brief elevation of IOP, which they call hypercompliance, they have found expansion of the anterior and posterior scleral, or neural, canal as compared to normal eyes and posterior deformation of the lamina cribrosa. Interestingly, while the laminar changes were most marked in the superior and inferior regions, significant deformations were present in all four quadrants of all three animals reported.

The power of this concept is that it not only includes the possibility that local variations in lamina cribrosa architecture can alter these stress/strain relationships, it also can be applied to progressive optic nerve damage. Here, these relationships will change with prolonged or fluctuating pressure as damage to the load-bearing structures occurs, due to progressive failure of the lamina cribrosa, presumably beginning with the anterior and thinnest laminar beams.¹¹

This theory also does not discriminate between the mechanical and vascular hypothesis, because these same concepts can be applied to the blood vessels within the laminar beams, thus affecting their patency, and the diffusion properties of the vessel walls. In fact, a recent report¹¹ indicates that capillary patency within the anterior laminar beams is diminished by high IOP in both normal eyes and those with early glaucoma. This is in agreement with earlier microsphere studies.⁵⁷ Further work by this group will focus on

refining the three-dimensional modeling of these relationships, including measurements of the material properties of the peripapillary sclera and lamina cribrosa. With this, they can develop a better understanding of how these properties change with progressive optic nerve damage.

An essential step in linking the biomechanical hypothesis to actual glaucomatous optic nerve damage, and hence to RGC axon injury, is to understand how stress/strain relationships get translated into the known cell biology of glaucomatous optic nerve damage. This thesis will help lay the groundwork for such an understanding.

INTEGRINS AND CELL ADHESION

Integrins are a family of membrane-spanning proteins that are important receptors for cell adhesion to ECM proteins. They also provide connections between the extracellular environment and the cell cytoskeleton and are responsible for activating many intracellular signaling pathways. In addition to their role with ECM, they are now known to mediate many cell-cell interactions, including those involved in inflammation, hemostasis, and cancer metastasis while others serve as cell receptors for viruses and bacteria.¹⁵

Integrins exist as heterodimers consisting of α and β subunits that interact noncovalently. At present, 18 α - and eight β - subunits are recognized and known to form 24 different heterodimers, although an additional six α - and one β - subunit are now suspected, based upon a survey of the human genome.^{15,58} The specific combination of subunits forming the heterodimer is felt to dictate to some degree the specificity of the ligand to which the integrin will bind, activating the intracellular portion of the integrin.

Each integrin subunit appears to have one or more ligands to which it can bind. In turn, the specificity of ligand recognition for any heterodimer will be influenced by the specific combination of subunits, and the relative affinity and availability of the ligand.⁵⁹ In general, integrin ligands can be classified into four groups: ECM, soluble, cell-cell, and pathogens and toxins.⁵⁸ A detailed discussion of all of these groups, as well as the specific mechanisms of integrin binding and ligand activation, is beyond the scope of this thesis.^{15,58-61} However, for the purpose of understanding their role in detecting stress and strain within the optic nerve head, integrins that bind components of the ECM are listed in Table 1. The studies to be presented below will investigate the presence of the majority of these within normal and glaucomatous optic nerve heads.

TABLE 1. INTEGRIN SUBUNITS AND THEIR EXTRACELLULAR MATRIX LIGANDS^{58,59}

INTEGRIN	LIGAND
$\alpha_1 \beta_1$	Collagen 1, 2, 4; laminin
$\alpha_2 \beta_1$	Collagen 1, 2, 4; laminin; chondroadherin
$\alpha_3 \beta_1$	Laminin; reelin; thrombospondin-1; (collagen 1; fibronectin)
α_4	β_1 Fibronectin; osteopontin
	β_7 Fibronectin
$\alpha_5 \beta_1$	Fibronectin, laminin
α_6	β_1 Laminin
	β_4 Laminin
$\alpha_7 \beta_1$	Laminin
$\alpha_8 \beta_1$	Fibronectin; tenascin; nephronectin
$\alpha_9 \beta_1$	Tenascin; collagen; laminin; osteopontin
$\alpha_{10} \beta_1$	Collagen
$\alpha_{11} \beta_1$	Collagen
α_v	β_1 Fibronectin; vitronectin
	β_3 Fibronectin; vitronectin; tenascin; osteopontin
	β_5 Vitronectin; bone sialic protein
	β_6 Fibronectin; tenascin
	β_8 Collagen; laminin; fibronectin

Each integrin subunit has a large extracellular component, a membrane-spanning region, and a short cytoplasmic component.⁶⁰ The globular head domain of the extracellular component contains the ligand binding site. Recent years have seen rapid progress in our understanding of the mechanisms of ligand binding, and it is becoming clear that much of this binding is dictated by the presence of minimal recognition amino acid sequences within the ligands. One example of this is the RGD (arg-gly-asp) sequence, which serves as the fibronectin and vitronectin receptor for α_4 , α_5 , α_8 , and α_v .^{58,59} Alternatively, α_1 , α_2 , α_{10} , and α_{11} serve as collagen-binding receptors, whereas α_3 , α_6 , and α_7 bind to laminin. As seen in Table 1, many integrin subunits can preferentially bind the same ligands.

For some ligands, more than one sequence exists, and binding can be further influenced by residues flanking the sequence, as well as the three-dimensional conformation of the ligand itself.⁵⁹

Through their cytoplasmic tails, integrins provide a transmembrane link between their contact with the ECM and the cellular cytoskeleton. Generally, this linkage occurs through the actin-based microfilament system, with the exception of the $\beta 4$ tail, which interacts via plectin with intermediate filaments in the cell.^{15,62}

The submembrane protein complexes with which the integrin tails interact form focal adhesions, which consist of over 50 proteins and are linked to the actin cytoskeleton. Studies show that integrin-mediated focal adhesions are highly dynamic and can grow or shrink, depending upon the force that they experience.¹⁴ Thus, application of force will increase the size of a focal adhesion and the cytoskeletal resistance to deformation, allowing cells to adapt to changing external stimuli. These mechanosensors can also be activated internally through contraction of the actin-based cytoskeletal motor, and the degree of activation will be influenced by the pliability of the ECM, such that a stiffer matrix may generate a stronger response.¹⁴ Integrin activation can also result from growth factor stimulation.⁶³

In addition to progressive accumulation of focal adhesions between the membrane and the cytoskeleton, integrin activation can also produce a complex variety of signal transduction events via molecules that interact with the cytoplasmic tails.⁵⁸ These signaling pathways are now known to include cell survival, cell replication, differentiation, and cell motility.¹⁵ Many intracellular signaling pathways triggered by integrins are similar to those stimulated by growth factors, and, in fact, activation by these factors in some instances is dependent on integrin binding to their ligands. This signal transduction aspect of integrin function makes them attractive mediators for the events of glaucomatous optic neuropathy, since many of these functions also appear to occur in glaucomatous optic nerve heads.

At present, only $\beta 1$ integrin has been described within the normal primate optic nerve head.⁶⁴ In glaucomatous eyes, there appears to be increased immunoreactivity in astrocytes surrounding blood vessels at the vitreal surface of these optic nerve heads. However, a systematic survey of this and the other pertinent integrin subunits is currently lacking.

HYPOTHESIS

The previous discussion suggests that the optic nerve head is the primary site of glaucomatous optic nerve damage, and that the structure and composition of the load-bearing structures of the optic nerve head can dictate the distribution of alterations in stress and strain induced by changes in IOP. Furthermore, substantial data on the cell biology of glaucomatous optic nerve damage and the response to elevated IOP suggest that glaucomatous optic nerve damage involves a wide range of tissue alterations. These include cellular migration, cell division, reorganization, and altered deposition of the ECM.

The biomechanical theory is capable of unifying these observations and suggests that these cellular responses can be set into motion by detecting altered stress and strain within the lamina cribrosa and peripapillary sclera. However, it is currently unknown exactly how these forces are transmitted into a cellular response within the optic nerve head.

Integrins provide attachment between cells and the ECM via focal adhesions.^{14,15,58} Because the cytoplasmic domain of these membrane-spanning molecules also contacts the cytoskeleton, they are well positioned to detect changes in the physical state of the ECM and induce the cell to respond to these changes. To date, though, relatively little has been published on the presence and distribution of integrins in the optic nerve head, their potential cells of attachment, and their responses in glaucoma.

Because many integrin subunits are capable of binding to more than one ligand, it is possible that most, if not all, integrin subunits could exist within the primate optic nerve head. However, it is anticipated that specific integrin molecules are more likely to be associated with different structures of the optic nerve head.

Based upon the known distributions of integrin ECM ligands within the optic nerve head, it is anticipated that $\alpha 1$, $\alpha 2$, and $\beta 1$ will be present within the collagen-containing laminar beams and peripapillary sclera. The presence of laminin within basement membranes would further suggest that $\alpha 1$, $\alpha 2$, $\alpha 3$, $\alpha 5$, $\alpha 6$, $\beta 1$, and $\beta 4$ would be found surrounding laminar beams and within blood vessels, primarily associated with astrocytes and vascular endothelium.

The available literature on the presence of integrins within the central nervous system provides further clues as to what specific distributions might be expected. Early investigations of $\beta 1$ integrin in the rat brain showed its presence within vascular structures, glial cells, and the pia mater.⁶⁵ Within the optic nerve head itself, only $\beta 1$ has been associated with blood vessels and surrounding astrocytes.⁶⁴ Within the central nervous system, $\alpha 1\beta 1$, $\alpha 3\beta 1$, $\alpha 5\beta 1$, and $\alpha 6\beta 1$ have previously been described in association with astrocytes,⁶⁶ and $\beta 4$ has also been noted in human astrocytes.⁶⁷ Cultures of human Mueller cells, a prominent glial cell in the retina, have also been shown to express $\alpha 1$, $\alpha 2$, $\alpha 3$, and $\beta 1$ subunits.⁶⁸ The $\alpha 6\beta 1$ integrin has been identified as the primary laminin-1 receptor in the retina,⁶⁹ and $\alpha 2\beta 1$ appears to mediate tractional force from retinal Mueller cells.⁶⁸

From labeling studies of retinal samples, alpha subunits associated with $\beta 1$ in blood vessels are likely to be $\alpha 3$, $\alpha 5$, $\alpha 6$, and αv .⁷⁰ Specifically, $\alpha v\beta 3$ and $\alpha 5\beta 1$ appear to have a specific role mediating sheer stress to vascular endothelial cells, helping to govern growth and orientation of focal adhesions between these cells and their underlying substrate.⁷¹ αv knockout mice fail to survive and demonstrate cerebral hemorrhage, suggesting an important role for this integrin in microvascular cell adhesion during development.⁷²

From these observations, it is anticipated that $\alpha 1$, $\alpha 2$, and $\beta 1$ subunits will be present with cells in the load-bearing, collagen-containing laminar beams and peripapillary sclera. In addition, $\alpha 1$, $\alpha 2$, $\alpha 3$, $\alpha 5$, $\alpha 6$, $\beta 1$, and $\beta 4$ should be associated with astrocytes distributed around laminar beams and possibly into the glial columns. Finally, vascular distribution of integrins would be expected to include $\alpha 1$, $\alpha 2$, $\alpha 3$, $\alpha 5$, $\alpha 6$, αv , $\beta 1$, and $\beta 4$ subunits.

In order to test these hypotheses, the presence and distribution of integrins in normal primate optic nerve heads were evaluated

using a battery of antibodies to integrin subunits that bind to various components of the ECM. Human optic nerve heads with glaucomatous optic nerve damage were also analyzed by immunohistochemistry to detect changes from the normal distribution. These results will be interpreted in the light of current understanding of integrin function to determine the most likely contribution of these molecules to glaucomatous optic nerve damage and the optic nerve head structures that play an integral role in nerve damage.

METHODS

Glaucomatous (N = 32 from 26 individuals) and control human eyes (N = 20) were obtained through the Glaucoma Research Foundation and the Oregon Lions Eye Bank. Mean age of glaucoma donors was 77 years, and mean time from death to freezing for this group was 14 hours. For normal human donors, these numbers were 71 years and 24 hours, respectively. Glaucoma diagnoses were determined from clinical histories and included primary open-angle glaucoma (N = 26), pigmentary glaucoma (N = 2), uveitic glaucoma (N = 1), neovascular glaucoma (N = 1), and angle-closure glaucoma (N = 2). The extent of optic nerve damage was categorized as mild, moderate, or severe by reported clinical assessment of the cup-to-disc ratio in conjunction with visual fields and disc photos, when available. Control eyes had no evidence of glaucoma or retinal pathology, and the optic nerve appeared normal by direct inspection under a dissecting microscope.

Normal adult rhesus monkey eyes (N = 14, aged 2 to 25 years old) were used to corroborate findings in normal human eyes. These nonhuman primate tissues were obtained from the Oregon Regional Primate Research Center and frozen within 3 hours of sacrifice. The much shorter time from death to freezing in these specimens helped to ensure the identification of more labile epitopes that might otherwise have been missed in the human specimens, which generally required a longer preparation time. The more rapid processing time also provided excellent morphology, allowing more accurate localization of the label with different antibodies to specific structures.

Human tissue analyses were approved by the OHSU institutional review board and conformed to HIPAA guidelines. All animal experiments were performed in accordance with the ARVO Statement for the Use of Animals in Ophthalmic and Vision Research.

Optic nerve heads, with attached retinas, were dissected, immersed in OCT, and immediately frozen in 2-methyl butane chilled in liquid nitrogen. Longitudinal sections were cut on a Reichert cryostat and stored frozen until needed for immunohistochemistry. All immunohistochemistry was performed in triplicate (three sections per slide) using the ABC technique with DAB chromagen as described below.

Antibodies to ECM ligands consisted of goat anti-type 1 collagen and anti-type 3 (1:500, Southern Biotech), rabbit anti-collagen 4 (1:2,500, Biodesign), rabbit polyclonal anti-GFAP (1:500, Santa Cruz), rabbit polyclonal anti-human vitronectin (1:500 for rhesus, 1:1,000 for human tissue) and anti-fibronectin (1:5,000) antibodies (A104 and A101, Gibco Brl), rat polyclonal anti-aggrecan (1:10,000, a gift from Kurt Doege, PhD, Shriners Hospital), rabbit anti-human tenascin (1:3,000, Telios), and rabbit polyclonal anti-human laminin (1:2,000, Telios).

Antibodies to integrin subunits included the following: rabbit anti-rat $\alpha 1$ polyclonal (1:1000, AB1934, Chemicon), mouse anti-human $\alpha 2$ monoclonal (1:500, A042, Telios), mouse anti- $\alpha 3$ and - $\beta 2$ monoclonals (both 1:500, A043 and A052, Oncogene Science), mouse anti- $\alpha 4$, anti- $\alpha 5$, and anti- $\alpha 6$ monoclonals (all 1:500, 0764, 0771, and 0769, AMAC), mouse anti-human αv , $\beta 1$, $\beta 3$, and $\beta 4$ monoclonals (all 1:500, MAB1980, MAB1977, MAB1974, and MAB1964, Chemicon), mouse anti-human $\beta 4$ (1:1,000, clone 3E1, Gibco), and mouse anti-human $\beta 2$ (1:1,000, Clone P4H9, Oncogene). All antibodies had been used in previously published immunoassays^{70,73} and were selected from a larger group of available antibodies based on the intensity of their staining pattern.

Slides were fixed in methanol at 4°C for 15 minutes followed by three washes in phosphate buffered saline (PBS). Slides were placed for 30 minutes in 20% normal serum in PBS with 1% bovine serum albumen (PBS/BSA) to block nonspecific binding. Primary antibodies (or appropriate nonimmune IgG or sera), diluted as indicated in PBS/BSA, were applied for 18 hours at 4°C, followed by wash in PBS. Biotinylated secondary antibodies (Vector Laboratories), diluted 1:200 in PBS/BSA, were applied for 30 minutes and then washed in PBS + 0.01% Triton x-100 (PBS/Triton). Avidin-biotin-peroxidase complex (Vector Laboratories), diluted 1:1,000 in PBS, was applied for 45 minutes, washed in PBS, followed by a wash in tris buffered saline, pH 7.2 (TBS). Chromagen was developed for 3 minutes in 0.05% 3,3-diaminobenzidine with 0.03% H₂O₂ in TBS and counterstained with hematoxylin, dehydrated and cover-slipped.

For controls, each immunoassay included sections from normal and glaucomatous eyes that were exposed to the complete immunohistochemical labeling process, but with appropriately diluted, normal sera or immunoglobulin substituted for the primary antibody.

All slides were independently evaluated using a Zeiss Axiophot light microscope by two or more observers who judged labeling intensity on a scale of 0 to 3. Specific structures evaluated for labeling were peripapillary sclera, laminar beams, laminar beam margins, glial columns anterior to the lamina cribrosa, capillaries of the lamina and prelamina, and larger blood vessels of the optic nerve head and peripapillary sclera. All findings were documented using a Leica DC 500 digital camera.

RESULTS

INTEGRIN LIGAND DISTRIBUTION IN THE NORMAL OPTIC NERVE HEAD

The normal distribution of the most common ECM integrin ligands were in agreement with previously published studies. These are summarized here and illustrated in Figure 2 to provide a framework with which to correlate the integrin findings.

Fibrillar collagen types 1 and 3 were diffusely distributed within the peripapillary sclera, the optic nerve sheath, the lamina

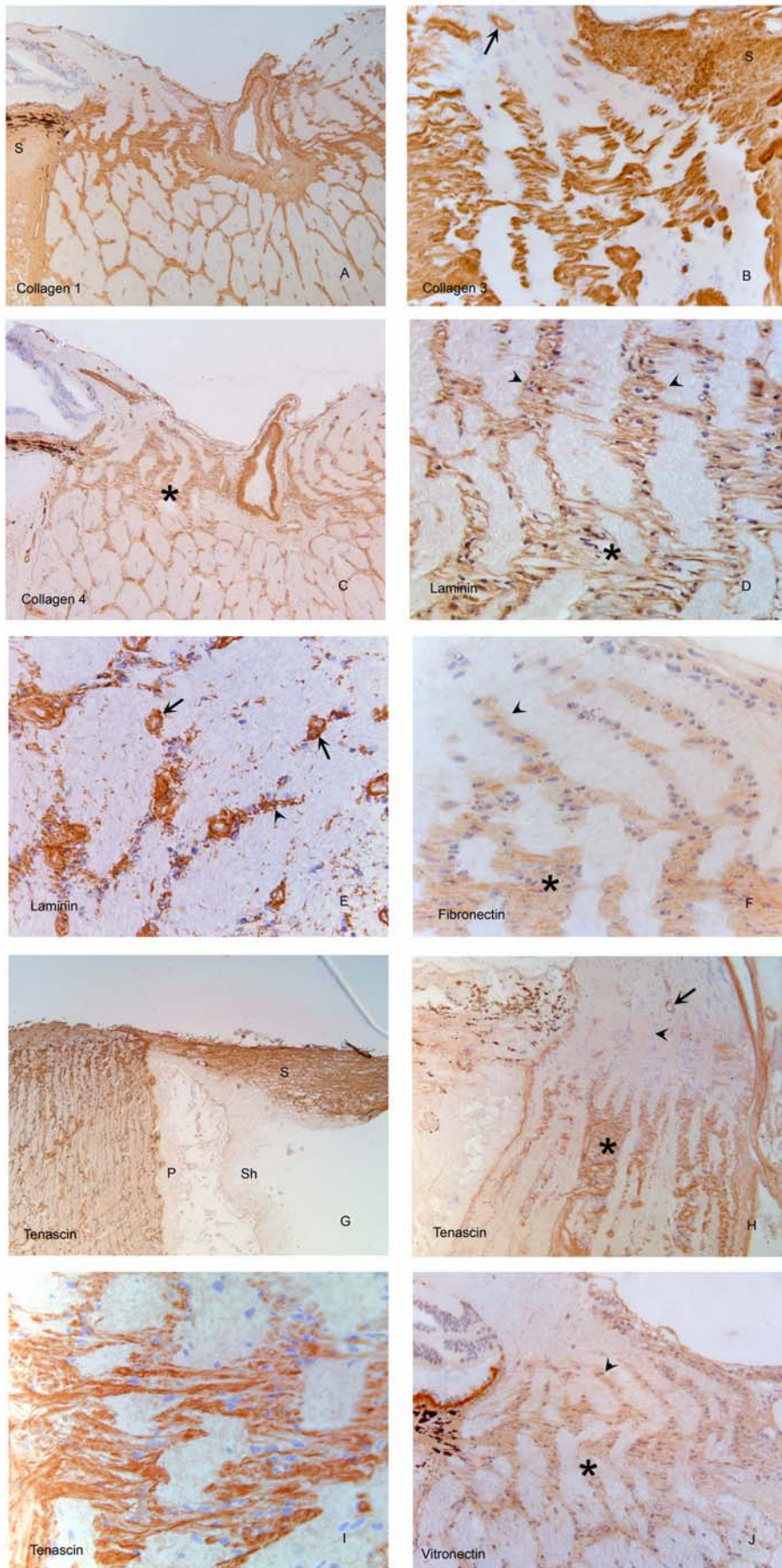


FIGURE 2

Distribution of common ECM integrin ligands within the normal primate optic nerve head. Antibodies to fibrillar collagens 1 (A) and 3 (B) demonstrate dense label of the collagenous inner portions of the lamellar beams, with little extension into the anterior region of the optic nerve head, except in association with blood vessels (arrow). Note lack of label in association with individual astrocytes in this region. Collagen 4 (C) and laminin (D) antibodies label the margins of the lamellar beams, (*) corresponding to basement membranes of the astrocyte foot processes. In contrast to the fibrillar collagens, both of these constituents, and in particular laminin, appear anterior to the collagenous lamina, tapering into the glial columns in association with blood vessels and astrocytes (arrowheads) (D and E). Fibronectin (F), which generally colabels with fibrillar collagens, also labels the collagenous lamellar beams as well as peripapillary sclera and major blood vessels, and is present over the glial columns anteriorly. Tenascin (G) demonstrates a very distinct label of the sclera (S) and peripapillary sclera, but not the optic nerve sheath (Sh) or pia (P), in distinction to the fibrillar collagens. Within the lamina cribrosa (*), tenascin labels the lamellar beams (H and I), but this does not extend anteriorly (arrowhead), except in association with blood vessels (arrow). Higher-power view (I) illustrates label of lamellar beams, without cellular label in between the individual beams. Label with vitronectin antibodies (J) was heavier over the anterior portions of the lamina and glial columns, with relatively less intense staining of the collagenous lamellar beams (*). (Magnification: A, $\times 68$; B, $\times 136$; C, $\times 68$; D, $\times 272$; E, $\times 272$; F, $\times 272$; G, $\times 17$; H, $\times 68$; I, $\times 272$; J, $\times 136$)

cribrosa beams, and the adventitia of the major blood vessels of the optic nerve and retina. Within the lamina cribrosa, these collagens do not extend into the anterior portions of the nerve head, except where they are in association with blood vessels (Figure 2A and 2B). Collagen type 4, a component of basement membranes, was present along the margins of the retrobulbar optic nerve septae and lamellar beams in astrocyte basement membranes, where they contact collagenous tissues. It was also found in the inner margins of the blood vessels, in basement membranes of the vascular endothelial cells (Figure 2C). Laminin, another basement membrane constituent, demonstrated a similar distribution (Figure 2D). Both also demonstrated significant label in association with the glial columns anterior to the lamellar beams, in between the axon bundles. As these columns extend anteriorly, the density of the label gradually tapered away, with decreasing density of the astrocyte nuclei, although prominent vascular label persisted (Figure 2E). Fibronectin, which is commonly codistributed with fibrillar collagens, also labeled similar tissues to the collagens of the lamellar beams, peripapillary sclera, and major blood vessels. However, this label also extended anterior to the lamina, in association with the glial columns (Figure 2F).

Two other major ligands for integrins, tenascin and vitronectin, were also present within the normal optic nerve head.^{50,74} Tenascin demonstrated a heavy label in the posterior sclera but, unlike the fibrillar collagens, did not extend to the pia of the optic nerve or the optic nerve sheath (Figure 2G). Within the lamina cribrosa, heavy label is also seen over the collagenous portions of the lamina cribrosa (Figure 2H and 2I). Vitronectin demonstrated the most intense label over the glial columns just anterior to the lamina, with relatively less label of the collagenous lamellar beams (Figure 2J). Here, too, posterior scleral tissues were found to label more heavily, with minimal label over the optic nerve sheath and optic nerve pia, posterior to the lamina cribrosa.

INTEGRIN DISTRIBUTION IN THE NORMAL OPTIC NERVE HEAD

Four patterns of distribution were seen for this battery of integrins with strong links to the ECM (Table 2). These were as follows: (1) minimal label, (2) label of vascular structures only, (3) label of lamellar margins, glial columns, and vasculature, and (4) label of lamellar margins and glial columns without label of vasculature. None of the antibodies demonstrated cellular staining of the peripapillary sclera, with the exception of blood vessels.

TABLE 2. RANGES OF INTEGRIN LABELING INTENSITIES IN NORMAL OPTIC NERVE HEADS

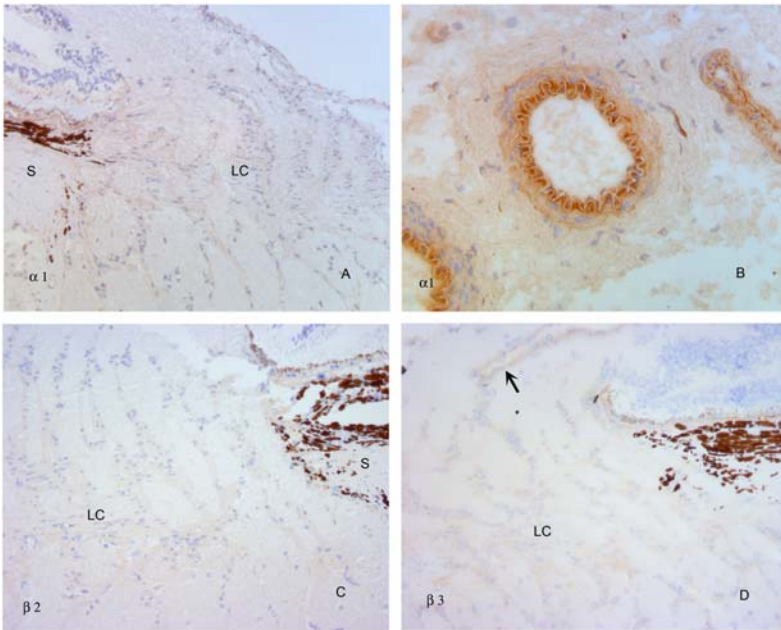
INTEGRIN	SCLERA	LC MARGINS	GLIAL COLUMNS	CAPILLARIES*	ARTERIES*
α_1	0	0 - 1.0	0 - 1.0	0 - 1.0	0 - 1.0
α_2	0	1.5 - 3.0	1.5 - 3.0	0 - 1.0	0 - 1.0
α_3	0	2 - 3	2 - 3	2.5 - 3.0	2.5 - 3.0
α_4	0	0 - 1	0 - 1	2 - 3 (discontinuous)	0
α_5	0	0 - 1	0 - 1	2.5 - 3.0	2.5 - 3.0
α_6	0	2.5 - 3.0	2.5 - 3.0	2.5 - 3.0	2.5 - 3.0
α_v	0	0 - 1	0 - 1	2 - 3	2 - 3
β_1	0	2.5 - 3.0	2.5 - 3.0	2.5 - 3.0	2.5 - 3.0
β_2	0	0 - 1	0 - 1	0 - 1	0
β_3	0	0	0 - 1.0	0	1.5 - 2.5 (intima)
β_4	0	2 - 3	2 - 3	2 - 3	2 - 3

LC, lamina cribrosa.

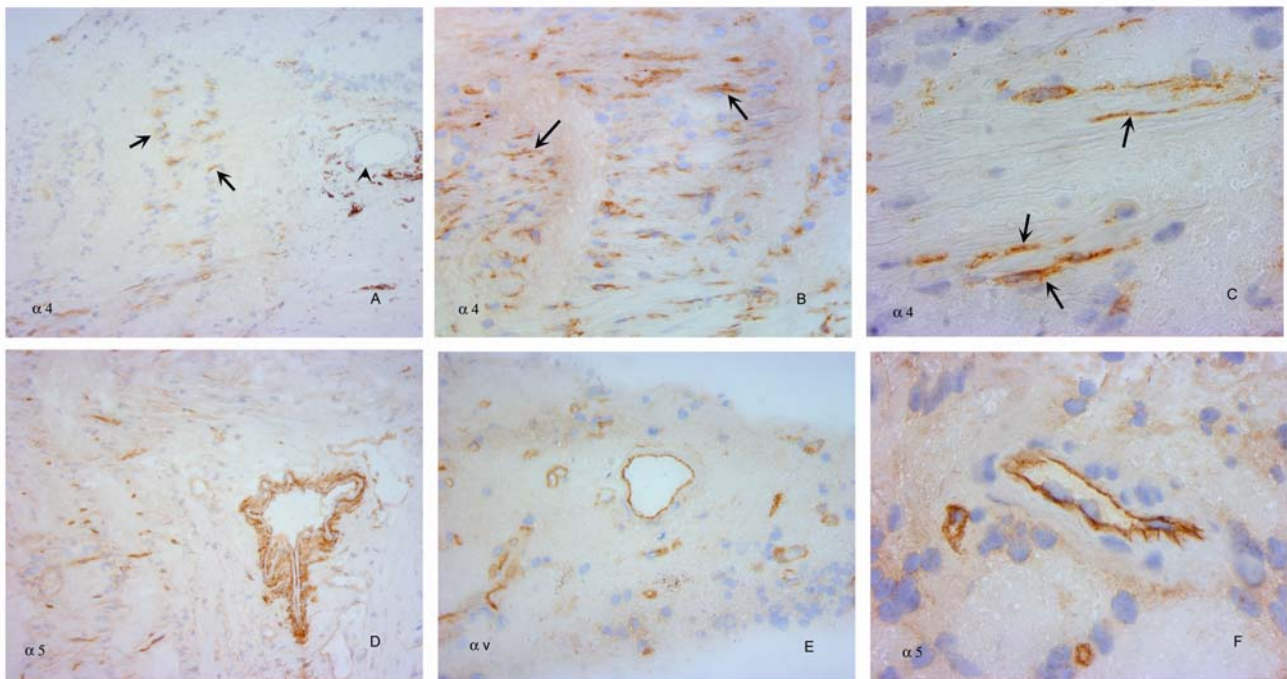
*Unless otherwise noted in parentheses, vascular labeling indicates endothelial pattern.

Antibodies to α_1 , β_2 , and β_3 failed to label the optic nerve head to an extent greater than that produced by controls (Figure 3A and 3C). Antibodies to α_1 only demonstrated moderate label of the intimal region of the arterioles within the peripapillary sclera (Figure 3B), and β_3 only produced light label of the larger arteries of the retina (Figure 3D).

α_4 , α_5 and α_v primarily labeled optic nerve head blood vessels (Figure 4). Of these, α_4 failed to label the larger blood vessels, either within the optic nerve head or in the peripapillary sclera (Figure 4A). In addition, the α_4 label pattern of the capillaries and small vessels was unique from that of the other two antibodies, since it had a patchy distribution along the vessel walls (Figure 4B and 4C). Antibodies to α_5 and α_v labeled both small and large vessels, with a more continuous label pattern, suggesting an endothelial basement membrane (Figure 4D, 4E, and 4F). In the larger vessels, this label also appeared to be associated with the vascular intima. There was little to no label of the glial columns or margins of the collagenous lamellar beams with any of these three antibodies.

**FIGURE 3**

$\alpha 1$, $\beta 2$, and $\beta 3$ integrins within the normal primate optic nerve head. Antibodies to $\alpha 1$ integrin demonstrate none to minimal specific label (A), with the exception of larger blood vessels of the peripapillary sclera (B). $\beta 2$ antibodies (C) failed to demonstrate label to any identifiable structure of the optic nerve head. $\beta 3$ antibodies (D) also failed to produce specific label, with the exception of large retinal vessel walls (arrow). S, sclera; LC, lamina cribrosa. (Magnification: A, $\times 136$; B, $\times 272$, C, $\times 136$, D, $\times 136$)

**FIGURE 4**

$\alpha 4$, $\alpha 5$ and αv integrins within the normal primate optic nerve head. Antibodies to $\alpha 4$ integrin (A) demonstrate only scattered label (arrows) within the lamina and prelaminar optic nerve head, without labeling an arteriole in the peripapillary sclera (arrowhead). Higher-power views of the lamina (B, C) illustrate discontinuous label of small vessels (arrows). $\alpha 5$ (D) and αv (E) antibodies produce strong label of the central retinal vessels and capillaries of the lamina cribrosa and anterior optic nerve head. High-power view (F) documents a continuous label pattern in contrast to the discontinuous pattern shown by $\alpha 4$ integrin. Similar findings were observed for αv (not shown). Label of lamina beam margins and glial columns was absent or minimal with all of these antibodies. (Magnification: A, $\times 136$; B, $\times 272$; C, $\times 680$; D, $\times 136$; E, $\times 272$; F, $\times 680$)

Labeling with the remainder of the integrin antibodies was dominated by a pattern consistent with astrocyte cell bodies of the optic nerve head. Of these, the $\alpha 2$ pattern was unique (Figure 5). Here, label of astrocyte cell bodies surrounded the individual plates of the lamina beams, with the heaviest label occurring just anterior to the collagenous lamina cribrosa, over with the heaviest concentration of astrocytes in the glial columns (Figure 5A and 5B). At this same level, there was a general increase in diffuse label

within the nerve bundles between the glial columns that extended up to the nerve fiber layer of the optic nerve head. However, the small vessels of the optic nerve head, as well as the larger vessels of the peripapillary sclera and central vessels, did not demonstrate significant label (Figure 5C), although concentrations of astrocyte nuclei could be seen labeled around individual vessels (Figure 5B).

$\alpha 3$ and $\alpha 6$ antibodies, as well as antibodies to $\beta 1$ and $\beta 4$, labeled the margins of the lamina cribrosa beams and extended into the glial columns (Figure 6A through 6F). However, in contrast to $\alpha 2$, these antibodies also labeled small blood vessels and larger arterioles with a continuous pattern similar to that seen with $\alpha 5$ and αv (Figure 6G and 6H).

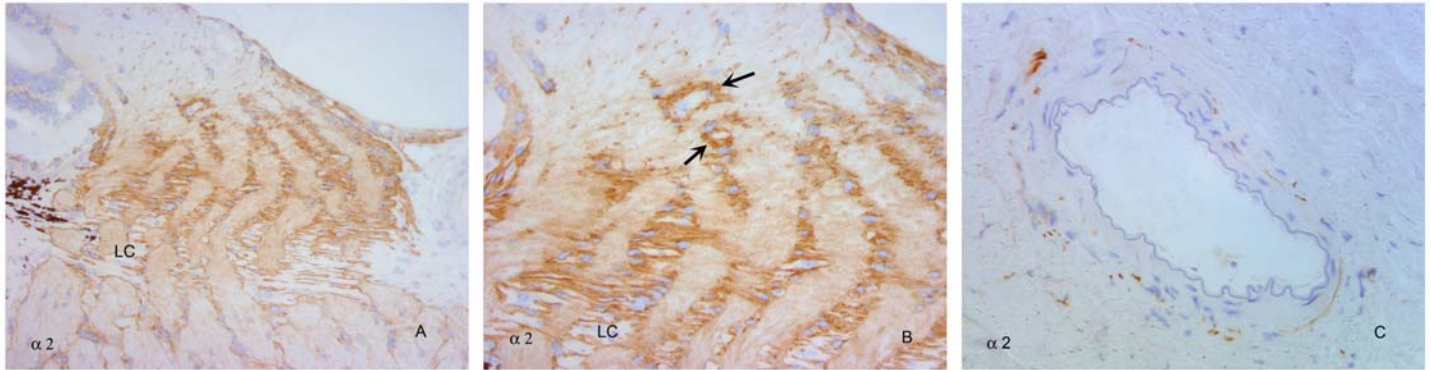


FIGURE 5

$\alpha 2$ integrins within the normal primate optic nerve head. $\alpha 2$ integrin antibodies (A) demonstrate label of astrocytes surrounding the collagenous laminar beams, with increased intensity over the glial columns just anterior to the laminar beams. Higher-power view (B) shows label around, but not within, laminar beams at lower part of micrograph, with label of astrocyte columns extending anteriorly, into the lamina choroidalis. Collections of astrocytes outline small blood vessels (arrows), which otherwise are not specifically labeled in the nerve fiber layer region of the optic nerve head. (C) Peripapillary arteriole not labeled with antibodies to $\alpha 2$. LC, lamina cribrosa. (Magnification: A, $\times 136$; B, $\times 272$; C, $\times 272$)

INTEGRIN LIGAND DISTRIBUTION IN GLAUCOMATOUS OPTIC NERVE HEADS

Glaucoma specimens were characterized by varying degrees of disorganization of the ECM structure of the optic nerve head. Those with severe injury demonstrated compression and posterior bowing of the lamina cribrosa, with loss of the normal lamellar pattern and filling in of the laminar pores, clearly demonstrated with antibodies to fibrillar collagens (Figure 7A and 7B). In addition, a cell layer was present anterior to the lamina in nearly all of these specimens, which in other studies was found to be composed of astrocytes.⁵⁰ While these cells labeled poorly with collagen antibodies, they demonstrated scattered label with tenascin, which more heavily labeled the laminar beams (Figure 7C and 7D). Vitronectin strongly labeled the anterior portions of the lamina cribrosa, with less intensity over the more posterior lamina (Figure 7E and 7F). Fibronectin label was diffuse in these specimens (not shown).

INTEGRIN DISTRIBUTION IN GLAUCOMATOUS OPTIC NERVE HEADS

Optic nerve heads with mild to moderate damage demonstrated disorganization of the laminar beams, but with relatively few alterations from expected integrin labeling patterns described for normal tissues (Figure 8). In severely injured eyes, cells anterior to and within the compressed lamina cribrosa demonstrated specific alterations in labeling patterns to some of the integrin subunits. Table 3 presents a summary of labeling patterns in normal vs glaucomatous specimens.

As in normal tissues, antibodies to $\alpha 1$, $\beta 2$, and $\beta 3$ integrin all failed to produce specific label in any of the damaged optic nerve heads. The only exception to this was $\beta 3$, in which label for the central retinal blood vessels noted in normal specimens persisted (Figure 9).

$\alpha 5$ and αv antibodies both produced the expected label of blood vessel margins (Figure 10). There was no significant increase in label of cells anterior to the compressed, bowed lamina cribrosa with either of these antibodies (Figure 10B and 10C).

By contrast, $\alpha 4$ antibodies demonstrated increased cellular label (Figure 11A through 11C). Whereas in normal optic nerve heads there was minimal label of laminar beam margins and the glial columns, the cells anterior to the lamina cribrosa showed definite label of these cells in most, but not all, of the heavily damaged specimens (Figure 11D). A similar increase in labeling intensity of cells within the lamina cribrosa could not be definitely determined (Figure 11B and 11C).

Antibodies to $\alpha 2$, $\alpha 3$, and $\beta 1$ all demonstrated strong anterior cellular label in specimens with severe damage from either primary or secondary glaucoma (Figure 12A through 12D and 13A through 13D). In contrast, cellular antibody labeling to $\alpha 6$ was relatively weak anterior to the lamina cribrosa, as compared to the strong label seen with these antibodies in the normal specimens (Figure 12E and 12F and Figure 13E). Label of laminar beam margins appeared unaffected.

$\beta 4$ antibodies demonstrated a variable response. In some eyes, cellular label anterior to the lamina cribrosa was heavy (Figure 14A through 14C), whereas in other, equally damaged eyes, label of this region was diminished (Figure 14D).

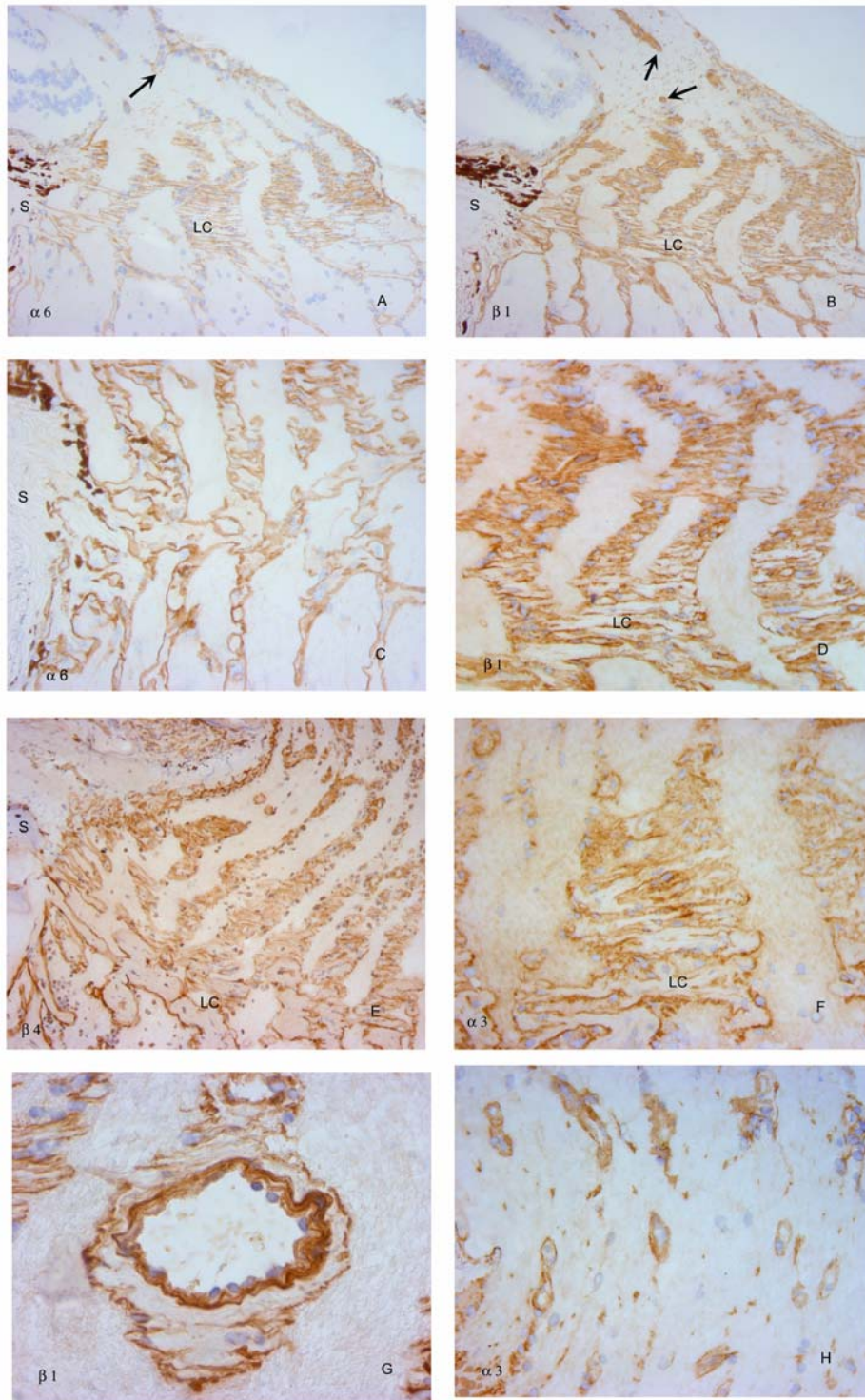


FIGURE 6

$\alpha 3$, $\alpha 6$, $\beta 1$, and $\beta 4$ integrin distribution within the normal primate optic nerve head is similar to that of $\alpha 2$, with the exception of the vasculature. Low-power micrographs (A and B) illustrate overall label of lamina beam margins, with heavier label over the glial columns, tapering anteriorly into the nerve fiber layer. Note label of vasculature in anterior optic nerve head (arrows). Higher-power views document label of lamina beam margins (C) and transition from lamina beams to glial columns (D, E, F). All antibodies labeled inner margins of blood vessels and capillaries within the lamina cribrosa (G) and those anterior to the lamina, extending into the nerve fiber layer (H). S, sclera; LC, lamina cribrosa. (Magnification: A, $\times 136$; B, $\times 136$; C, $\times 272$; D, $\times 272$; E, $\times 136$; F, $\times 272$; G, $\times 680$; H, 272)

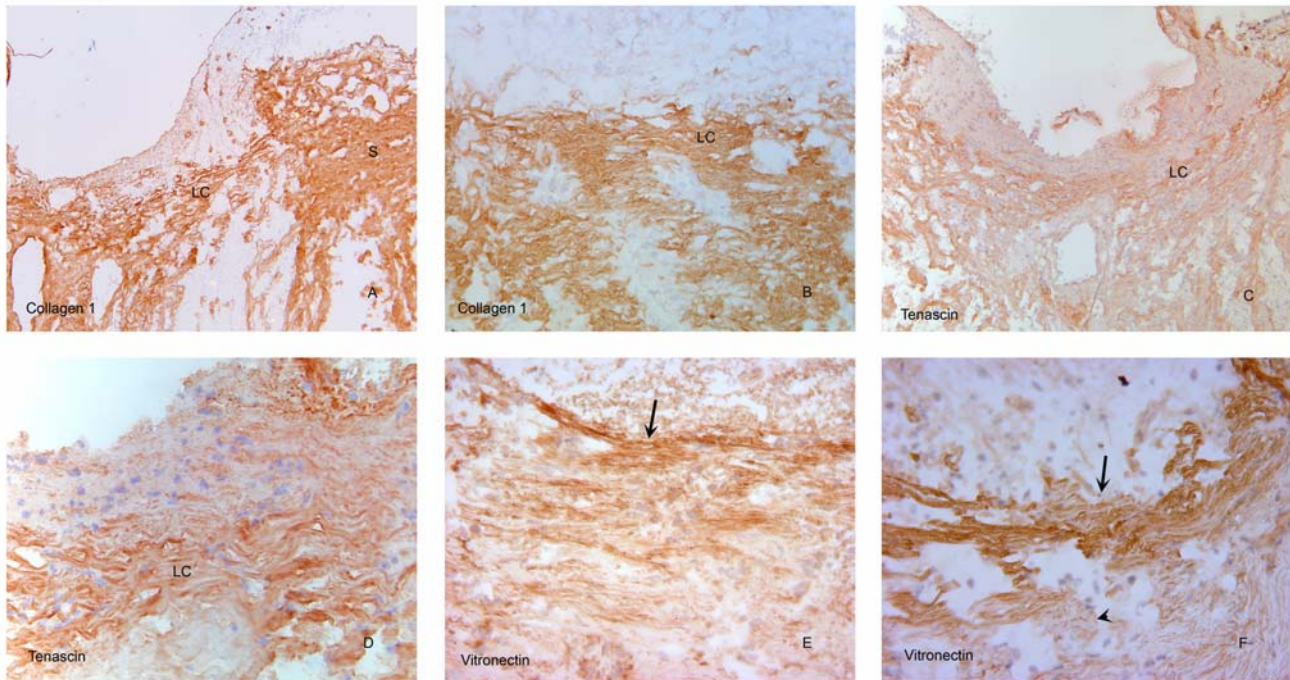


FIGURE 7

ECM integrin ligands in glaucomatous optic nerve damage. Collagen 1 label in an eye with severe optic nerve damage from primary open-angle glaucoma (A and B). Note condensed lamina cribrosa (LC), with loss of normal layered architecture and unlabeled cellular layer anterior to the lamina. Tenascin antibody label (C and D) is primarily restricted to the compressed lamina cribrosa in a similarly damaged eye, with relatively little cellular label within, and anterior to the lamellar beams. Vitronectin label appears most intense (arrows) over the anterior lamellar beams in an eye with primary open-angle glaucoma (E) and neovascular glaucoma (F). Arrowhead in F indicates less intense label of posterior lamina cribrosa. S, sclera. (Magnification: A, $\times 68$; B, $\times 272$; C, $\times 68$; D, $\times 272$; E, $\times 272$; F, $\times 272$)

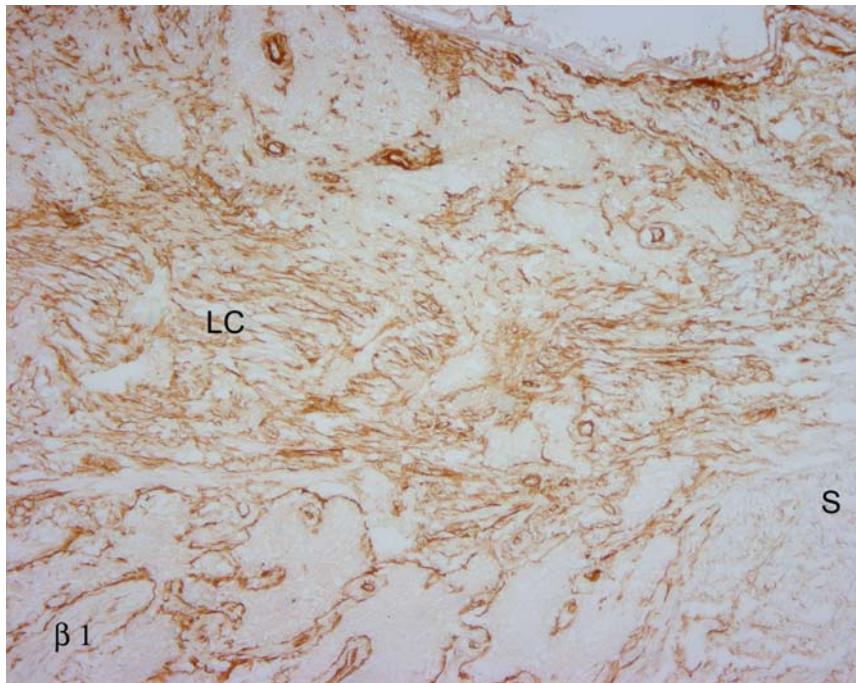


FIGURE 8

Label of eye with moderate glaucomatous optic nerve damage using antibodies to $\beta 1$ integrin. Note general disorganization of normal lamellar structure and poor delineation of lamina cribrosa (LC). (Magnification $\times 68$)

TABLE 3. RANGES OF INTEGRIN LABELING INTENSITIES IN NORMAL AND GLAUCOMATOUS OPTIC NERVES

INTEGRIN	STRUCTURE	NORMAL	GLAUCOMA
α_1	Laminar margins	0 - 1	0 - 1
	Glial columns/prelaminar cells	0 - 1	0 - 1
	Capillaries	0 - 1	0 - 1
α_2	Laminar margins	1.5 - 3.0	1.5 - 3.0
	Glial columns/prelaminar cells	1.5 - 3.0	1.5 - 3.0
	Capillaries	0 - 1	0 - 1
α_3	Laminar margins	2 - 3	2 - 3
	Glial columns/prelaminar cells	2 - 3	2 - 3
	Capillaries	2.5 - 3.0	2.5 - 3.0
α_4	Laminar margins	0 - 1	0 - 1
	Glial columns/prelaminar cells	0 - 1	1 - 3
	Capillaries	2 - 3 (discontinuous)	2 - 3 (discontinuous)
α_5	Laminar margins	0 - 1	0 - 1
	Glial columns/prelaminar cells	0 - 1	0 - 1
	Capillaries	2.5 - 3.0	2.5 - 3.0
α_6	Laminar margins	2.5 - 3.0	2.5 - 3.0
	Glial columns/prelaminar cells	2.5 - 3.0	0 - 2
	Capillaries	2.5 - 3.0	2.5 - 3.0
α_v	Laminar margins	0 - 1	0 - 1
	Glial columns/prelaminar cells	0 - 1	0 - 1
	Capillaries	2 - 3	2 - 3
β_1	Laminar margins	2.5 - 3.0	2.5 - 3.0
	Glial columns/prelaminar cells	2.5 - 3.0	2.5 - 3.0
	Capillaries	2.5 - 3.0	2.5 - 3.0
β_2	Laminar margins	0 - 1	0 - 1
	Glial columns/prelaminar cells	0 - 1	0 - 1
	Capillaries	0 - 1	0 - 1
β_3	Laminar margins	0	0
	Glial columns/prelaminar cells	0 - 1	0 - 1
	Capillaries	0	0
β_4	Laminar margins	2 - 3	2 - 3
	Glial columns/prelaminar cells	2 - 3	1 - 3
	Capillaries	2 - 3	2 - 3

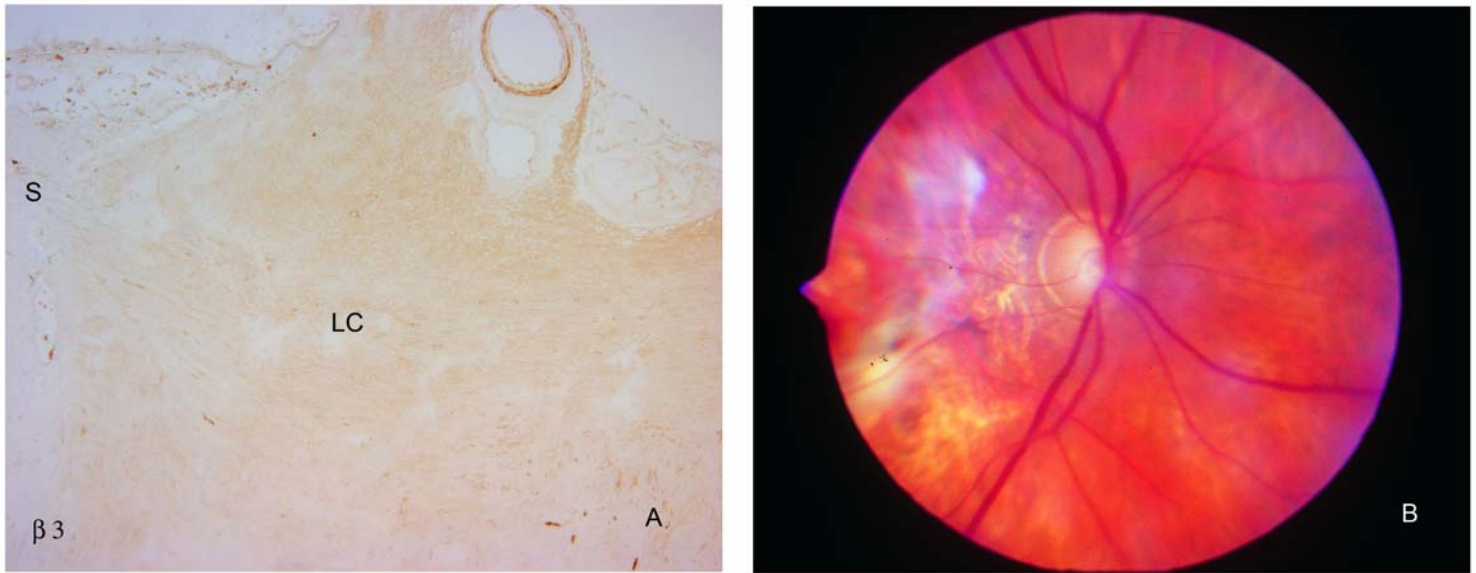


FIGURE 9

$\alpha 1$, $\beta 2$, and $\beta 3$ integrin labeling of cells in the optic nerve head is not altered in glaucoma. As illustrated for $\beta 3$ (A), antibodies to these integrins do not specifically label lamina cribrosa (LC) region of the optic nerve head from an eye with extensive optic nerve damage. Note labeling of central retinal vessel at top of photograph, as also observed in normal eyes. A clinical photograph of this eye is shown in (B). S, sclera; LC, lamina cribrosa. (Magnification: A, $\times 68$)

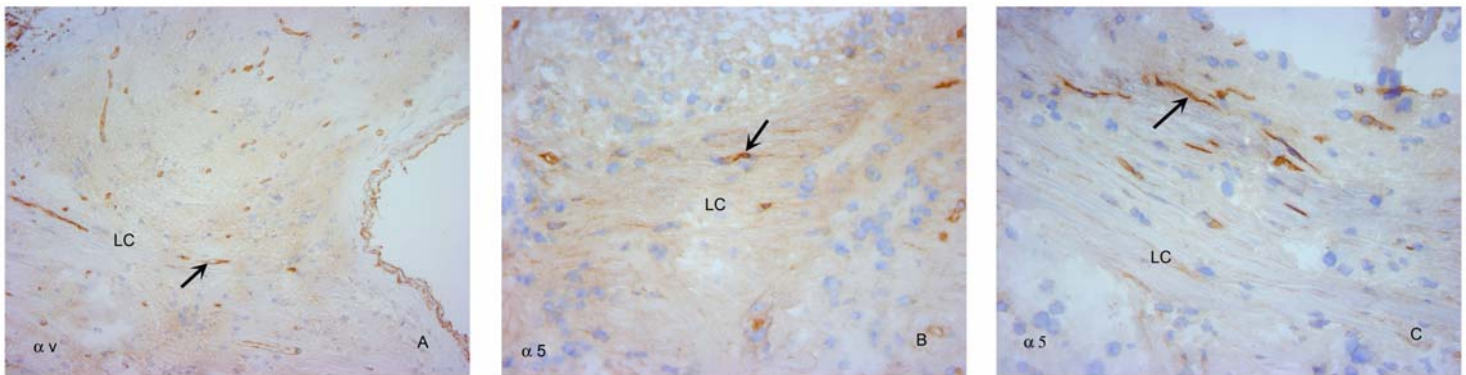


FIGURE 10

Vascular labeling with αV and $\alpha 5$ integrin antibodies is not altered in glaucomatous optic nerve heads. Antibodies to αv (A) and $\alpha 5$ (B) produced expected label of blood vessels only (arrows) in optic nerve head from specimen shown in Figure 9. Similar pattern with antibodies to $\alpha 5$ in another specimen with advanced glaucomatous injury is seen in C. Label of cells anterior to the compressed lamina cribrosa is nearly absent. LC, lamina cribrosa. (Magnification: A, $\times 68$; B, $\times 272$; C, $\times 272$)

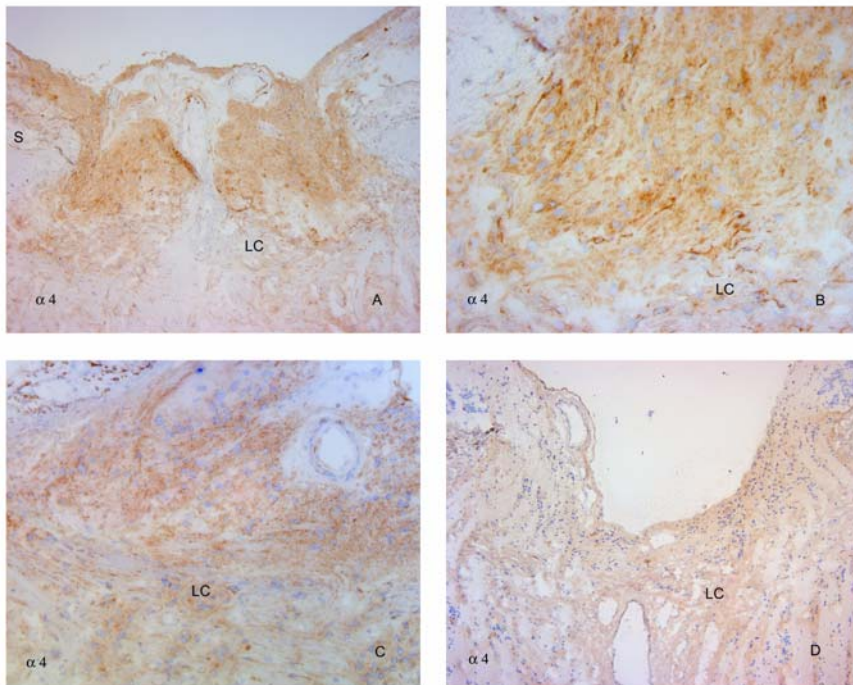


FIGURE 11

Glaucomatous damage intensifies $\alpha 4$ labeling anterior to the lamina cribrosa. Antibodies to $\alpha 4$ reveal intensified label of cells anterior to the lamina cribrosa in an eye with severe nerve damage from neovascular glaucoma (A and B) and in a specimen with primary open-angle glaucoma (C), also shown in Figure 9C. However, in a third eye with advanced cupping from primary open-angle glaucoma (D), label intensity was not dramatically increased. Label intensity of cells within the lamina cribrosa was relatively minimal and not noticeably altered from that in normal tissues. S, sclera; LC, lamina cribrosa. (Magnification: A, $\times 68$; B, $\times 272$; C, $\times 136$; D, $\times 68$)

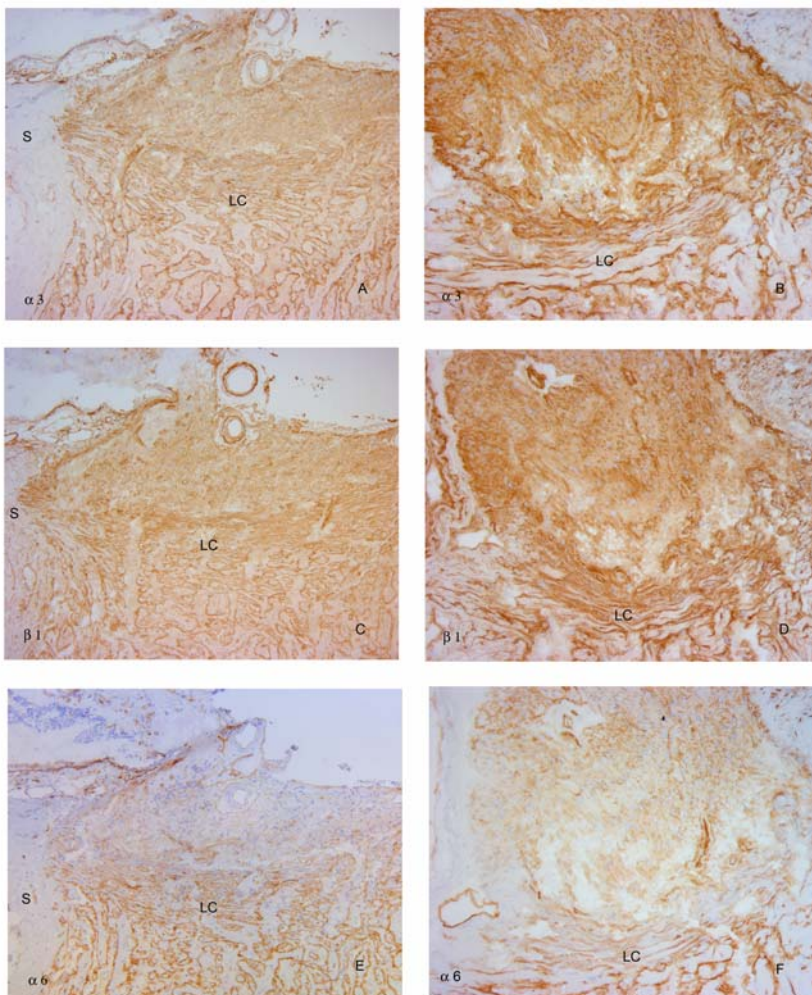


FIGURE 12

Glaucomatous damage does not affect prelaminar labeling with $\alpha 3$ and $\beta 1$ integrin antibodies but decreases label intensity for $\alpha 6$ integrin. Comparative label with antibodies to $\alpha 3$ (A and B), $\beta 1$ (C and D), and $\alpha 6$ (E and F) in optic nerve head from two glaucomatous eyes, one with extensive damage from primary open-angle glaucoma (A, C, E) and one with neovascular glaucoma (B, D, F). $\alpha 3$ and $\beta 1$ showed strong label of cells anterior to and between the compressed, posteriorly bowed lamina cribrosa in both specimens. In contrast, $\alpha 6$ label of prelaminar cells was surprisingly weak, whereas that between the laminar beams was similar to that in normal eyes. S, sclera; LC, lamina cribrosa. (Magnification: A, $\times 68$; B, $\times 136$; C, $\times 68$; D, $\times 136$; E, $\times 68$; F, $\times 136$)

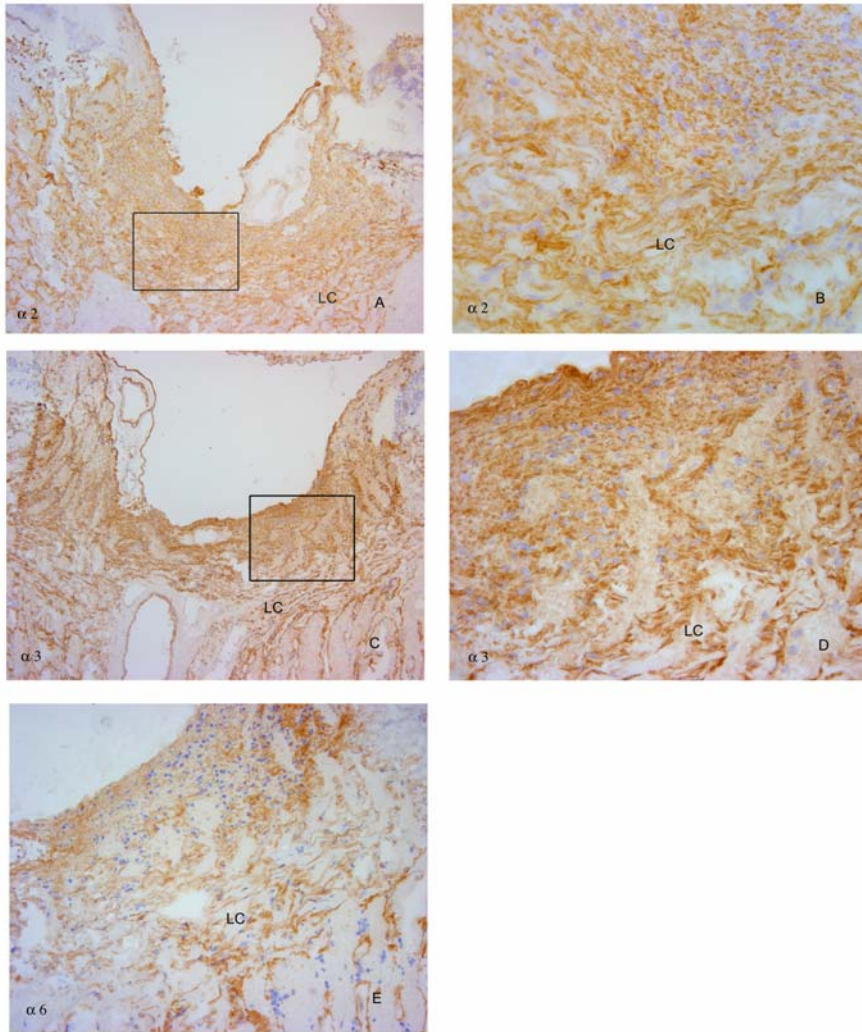


FIGURE 13

Prelaminar labeling with $\alpha 2$ and $\alpha 3$ antibodies in glaucomatous eyes is unaffected, in contrast to diminished intensity of $\alpha 6$. Two additional eyes with advanced damage from primary open-angle glaucoma demonstrate heavy cellular label with antibodies to $\alpha 2$ (A and B) and $\alpha 3$ integrin (C and D). $\alpha 6$ antibody label (E) was again reduced, although not completely absent in one of these specimens. LC, lamina cribrosa. (Magnification: A, $\times 136$; B, $\times 272$; C, $\times 68$; D, $\times 272$; E, $\times 136$)

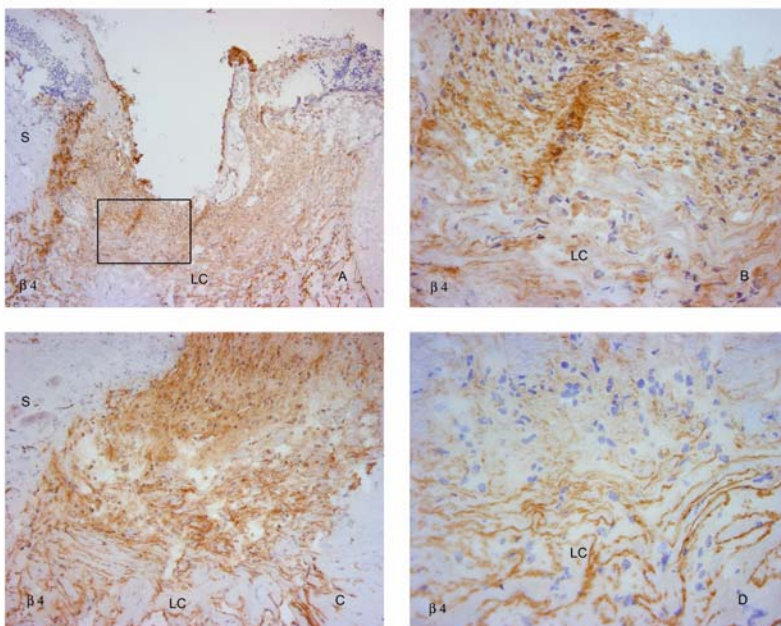


FIGURE 14

$\beta 4$ integrin in glaucomatous eyes. Label with antibodies to $\beta 4$ demonstrated variable patterns, with heavy anterior cellular labeling in an eye with advanced primary open-angle glaucoma (A and B) and in another with neovascular glaucoma (C). Label was markedly diminished in another with primary open-angle glaucoma damage (D). S, sclera; LC, lamina cribrosa. (Magnification: A, $\times 68$; B, $\times 272$; C, $\times 136$; D, $\times 272$)

DISCUSSION

Prior studies of integrin distribution in the posterior pole in primate eyes have primarily concentrated on retinal findings. Using a similar battery of antibodies, Brem and colleagues⁷⁰ found evidence for the presence of $\alpha 3$, $\alpha 5$, $\alpha 6$, αv , $\beta 1$, $\beta 2$, $\beta 3$, and $\beta 4$ in retinal blood vessels. Reduced or undetectable label of vessels with antibodies to $\alpha 2$ and $\alpha 4$ in normal eyes was consistent with the current study. In addition to vascular staining, $\alpha 2$, $\alpha 3$, $\alpha 4$, $\alpha 5$, and $\beta 2$ were found within the neural retina. Although there were no specific observations about astrocyte staining in this study, the internal limiting membrane, which is composed in part by Mueller cell end-feet and contains laminin and fibronectin, was positive for $\alpha 2$, $\alpha 3$, $\beta 1$, and $\beta 2$. Considering the wide range of integrin effects, these observations have major significance for several ocular neovascular diseases. A related study of proliferative retinal membranes demonstrated prominent label for $\alpha 6$ and $\beta 1$ in most membranes due to proliferative diabetic retinopathy and proliferative vitreoretinopathy, and expression for all subunits evaluated in vessels of membranes from proliferative diabetic retinopathy, as well as $\alpha 4$, which labeled normal vessels poorly.⁷³

To date, however, description of integrins in the optic nerve head has been limited to the observation of $\beta 1$ integrin in association with blood vessel walls and their surrounding astrocytes in the prelamina.⁶⁴ In glaucomatous optic nerve heads, $\beta 1$ label appeared to be increased in association with perivascular astrocytes immediately adjacent to the vitreous cavity. The current study thus represents the first systematic survey of the presence and distribution of the majority of integrin subtypes in the human and nonhuman primate optic nerve head.

INTEGRIN LABELING IN THE NORMAL OPTIC NERVE HEAD

Based upon known ligand affinities for the various integrin subunits and current data on integrin distribution within the central nervous system, it was anticipated that nearly all of the integrin subunits known to bind to the ECM would be present in the normal optic nerve head, representing several specific patterns. These expectations included (1) the presence of $\alpha 1$, $\alpha 2$, and $\beta 1$ subunits within cells of the load-bearing, collagen-containing lamellar beams and peripapillary sclera; (2) the association of $\alpha 1$, $\alpha 2$, $\alpha 3$, $\alpha 5$, $\alpha 6$, $\beta 1$, and $\beta 4$ with astrocytes around lamellar beams and possibly into the glial columns; and (3) the distribution of $\alpha 1$, $\alpha 2$, $\alpha 3$, $\alpha 5$, $\alpha 6$, αv , $\beta 1$, and $\beta 4$ subunits in capillaries and arterioles, most likely representing attachment of vascular endothelial cells to their basement membranes. Whereas the current findings support many of these predictions, certain discrepancies did surface, which help to clarify some events of glaucomatous optic neuropathy.

Antibodies to $\alpha 1$, $\beta 2$, and $\beta 3$ subunits produced relatively little label in any of the structures of the optic nerve head, with the possible exception of $\beta 3$, which appeared within the wall of the larger blood vessels. The $\beta 2$ subunit is primarily cellular and generally involved in leukocyte function, and this relative absence was not unexpected. Lack of label within glaucomatous optic nerve heads could indicate that immune mechanisms may not be contributing significantly to the injury process in the specimens studied here.

Another striking finding was the essential lack of cellular label within the collagenous core of the lamina cribrosa and the peripapillary sclera by antibodies to any of the integrin subunits. This relative lack of integrin presence would suggest that these putative load-bearing structures within the optic nerve head may not actively respond to fluctuations of IOP, and instead play a passive role in the glaucomatous nerve damage. This is further supported by a similar lack of label in either structure in even the most heavily damaged glaucoma specimens.

In contrast to the core of the lamellar beams, cells along the margins of the beams and within the glial columns labeled prominently with antibodies to $\alpha 2$, $\alpha 3$, $\alpha 6$, $\beta 1$, and $\beta 4$. This pattern is nearly identical to that previously noted for basement membrane constituents laminin and collagen 4 and illustrated in Figure 2.²⁸⁻³³ From this, it appears that the most likely cells labeled in this fashion are astrocytes, which line the lamellar beams, resting on a basement membrane that is interposed between them and the fibrillar collagen.

It is not possible to know exactly which integrin dimers are represented in a cell, based upon labeling patterns of individual subunits. However, integrin expression in astrocytes has been described before, and several members of the $\beta 1$ subclass have been described in the rat central nervous system, including $\alpha 1\beta 1$, $\alpha 3\beta 1$, $\alpha 5\beta 1$, and $\alpha 6\beta 1$.⁶⁶ Human Mueller cells, prominent glial cells in the retina, grown in culture have been shown to express $\alpha 1$, $\alpha 2$, $\alpha 3$, and $\beta 1$ subunits.⁶⁸ In addition, $\alpha 6\beta 4$, most widely known for its association with epithelial hemidesmosomes, has been described in nonhuman primates, where it is directly associated with astrocytes and their attachment to cerebral vascular walls.⁷⁵ $\beta 4$ has also been described in human astrocytes.⁶⁷ On the basis of this, it is likely that the integrin dimers found within the astrocytes of the optic nerve head in this study are $\alpha 2\beta 1$, $\alpha 3\beta 1$, $\alpha 6\beta 1$, and $\alpha 6\beta 4$. However, additional study using specific dimer antibodies would be necessary to confirm this interpretation.

All of these subunits have binding capabilities to laminin (Table 1), a prominent constituent of basement membranes. While basement membranes are less common in the glial columns, there appear to be significant amounts of both collagen 4 and laminin associated with these cells, as shown in Figure 2C and 2D. Thus, it is likely that this integrin label represents cell surface binding to these ECM materials in this region as well.

With the exception that neither $\alpha 1$ nor $\alpha 5$ were present, the observed integrin label pattern for astrocytes was nearly as predicted. The heavy representation of integrins in association with astrocytes of the optic nerve head clearly suggests that these cells can play an important role in glaucomatous injury⁶⁴ and is consistent with the possibility that these cells are equipped to detect stress within and anterior to the lamina cribrosa.

These results also showed that antibodies to $\alpha 2$, $\alpha 3$, $\alpha 5$, $\alpha 6$, αv , $\beta 1$, and $\beta 4$ were all associated with blood vessels. With the exception that no label with $\alpha 1$ antibodies was seen, this almost completely conformed to the predicted pattern. With the exception of $\alpha 2$, which appeared to be limited to perivascular astrocytes, vascular label with all of these antibodies was linear along the inner

margin of the vascular walls, highly suggestive of a vascular endothelial pattern. All of the α subtypes can dimerize with $\beta 1$ to form laminin receptors, with the exception of $\alpha \nu \beta 1$, which binds fibronectin. Because both laminin and fibronectin are present in basement membranes, it is likely that these integrins are important for attachment of endothelial cells to their basement membrane. It is also possible that many of these integrins are also labeling astrocytes that are in close apposition to vascular walls, as noted above for $\alpha 6 \beta 4$ integrin, which also binds laminin. Although the apparent lack of label of $\alpha 2$, which can also bind laminin, to vascular endothelium would seem inconsistent with this interpretation, it is known that integrin subunit binding is influenced by many factors, and expression can be variable from one cell type to another.⁶⁰

It is of interest that $\alpha 4$ was also found associated with blood vessels, but in a nonlinear, discontinuous pattern. It is possible that this discontinuous pattern with $\alpha 4$ represents labeling of microglia. A previous description of normal and glaucomatous human eyes studied by immunohistochemistry for microglia demonstrated labeled cells in the wall of blood vessels and capillaries in both the glial columns and the lamina cribrosa.⁷⁶ This pattern looks remarkably similar to that seen with $\alpha 4$ antibodies in the present study.

INTEGRIN LABELING IN GLAUCOMATOUS OPTIC NERVE HEADS

In eyes with glaucomatous optic nerve damage, the basic distribution of many of these integrins was maintained but reflected the remodeling of the optic nerve head. However, there was evidence that some of these subtypes responded in unexpected ways. This may reflect unique responses and potentially significant roles for some of these integrins in the damage process.

Two integrin subunits demonstrated a clear difference in their distribution in glaucomatous specimens, as opposed to the normal distribution. Notably, $\alpha 4$ appeared to be more prominent over nonvascular cells, primarily anterior to the compressed lamina cribrosa, and $\alpha 6$ demonstrated reduced label in this same region as compared to the density of label seen over glial columns in normal specimens. By contrast, Hernandez and associates⁵⁴ have reported a decrease of both subunits in their microarray analysis of cultured astrocytes from glaucomatous tissue.

The marked increase in label to $\alpha 4$ in glaucomatous specimens noted here could represent hypertrophy and multiplication of microglia, activated by optic nerve head damage. The activation and proliferation of these cells and their phagocytic roles, which involve movement of their processes through the neural parenchyma, likely involve disruption of existing integrin attachments to the ECM and the formation of new ones. This must be part of the remodeling and scarring process. In support of this possibility, microglia have been described to express $\alpha 4$, $\alpha 5$, and $\alpha \nu$,^{77,78} which are increased in activated microglia, and $\beta 1$ has been shown to participate in proliferation and chemotaxis of microglia on fibronectin.⁷⁹

Alternatively, when dimerized with $\beta 1$, $\alpha 4$ binds to fibronectin. Recently, it has been found that when porcine trabecular meshwork cells are stretched, this results in induction of message for alternatively spliced forms of fibronectin, which contain the capacity for more $\alpha 4 \beta 1$ binding sites (Gregory K, Association for Research in Vision and Ophthalmology, 2005, Abstract 1341). Although similar experiments have yet to be performed on astrocytes, such a change, occurring in response to elevated IOP, could also explain the increased presence of $\alpha 4$ labeling seen in these glaucomatous optic nerve heads.

The finding of reduced label with $\alpha 6$ antibodies presents another interesting response, in light of the previously mentioned $\alpha 6 \beta 4$ association between astrocytes and vascular walls of cerebral blood vessels. Working with a model of cerebral ischemia and reperfusion in nonhuman primates, Wagner and colleagues^{75,80} demonstrated that ischemia was followed within 2 hours by a reduction in expression for $\alpha 6$ and $\alpha 6 \beta 4$ integrin. This suggests that $\alpha 6 \beta 4$ mediates astrocyte-matrix interactions, which can become disrupted by ischemia. It is possible that a similar disruption involving this integrin dimer is occurring in optic nerve heads with glaucoma, thus reducing label for the $\alpha 6$ subunit. Whereas $\beta 4$ label of cells was present in many of these glaucoma specimens, this label was variable and may reflect a similar process.

Overall, the patterns of integrin label in eyes with primary open-angle glaucoma were similar to those seen in eyes with secondary glaucoma (Figure 12 and 13). This would suggest that the responses observed are relatively generalized and further support the concept that they represent the response of the optic nerve head to altered stresses from elevated IOP, as opposed to inherent differences in the cell biology of specific types of glaucoma.

POTENTIAL FUNCTIONS OF INTEGRINS IN GLAUCOMATOUS OPTIC NERVE DAMAGE

Glaucomatous optic neuropathy involves extensive remodeling of the optic nerve head. This includes evidence of astrocyte migration and shape change, the elaboration of matrix metalloproteinases, new synthesis and deposition of ECM materials, and cell division. Furthermore, there is increasing evidence that many of these changes can occur with astrocytes.⁶⁴ Because many of the integrin subunits identified in this study, both α and β , were identified in association with astrocytes of the optic nerve head, it is also reasonable to consider these functions in light of their potential contribution to glaucomatous optic nerve damage.

With regard to cell migration, integrin interactions between the cytoskeleton and the ECM provide attachments of the cell for its substrate to allow it to move.⁸¹ However, cell migration also depends upon a coordinated series of events, including the polymerization and depolymerization of the cytoskeleton, which are regulated by signaling pathways. Because many of these mechanisms can also be influenced by integrins, integrins are thus capable of affecting migration through both signaling and structural mechanisms.⁸²

The ability of integrins to set in motion other signaling pathways provides a wide range of additional effects in glaucomatous optic nerve heads. These include the ability of integrins to recruit and activate matrix metalloproteinases, key steps in the dissolution of the ECM, which then would allow migration of cells inherent in tissue remodeling.⁸³ Integrins can also promote cell proliferation, which can occur via integrin activation of AKT- and ERK-dependent G1 phase progression and induction of cyclin D1,⁸⁴ both of which have

been described in optic nerve heads following elevated IOP (Johnson E, Association for Research in Vision and Ophthalmology, 2005, Abstract 1243).

The localization of several integrins over the vascular endothelium and perivascular astrocytes in this study raises the possibility that these molecules may also mediate vascular changes in glaucomatous optic nerve damage. This has been previously considered by Burgoyne,¹¹ who postulated that tensile strain within laminar beams might induce basement membrane thickening by endothelial cells as well as astrocytes, and thus reduce nutrient diffusion from capillaries to the axon bundles. There is ample evidence supporting active roles for integrins in the pathology of the vasculature of the CNS.^{75,85-88}

MOLECULAR EVIDENCE FOR REGIONAL DIFFERENCES IN STRESS AND STRAIN WITHIN THE OPTIC NERVE HEAD

Finally, this study provides several interesting molecular clues to the existence of regional differences in stress and strain within the normal optic nerve head. Perhaps the most striking of these are the distinct location of tenascin and vitronectin for the peripapillary sclera and lamina cribrosa in the normal eye, with none over the pia and optic nerve sheath of the retrobulbar optic nerve (Figure 2G through 2J).

Tenascin-C is known to be heavily expressed at sites of high stress, such as tendons and ligaments.⁸⁹ It can also be induced in remodeling and wound repair in bone and skin⁹⁰ by cyclic tension.⁹¹ Among its many roles, tenascin can modulate adhesion of cells to fibronectin and has recently been shown to up-regulate in cells following injury in a scratch wound assay of cultured astrocytes, along with an increase of $\beta 1$ integrin.⁹² Thus, tenascin could contribute to proliferation and migration of astrocytes. Interestingly, in this experiment, while cells adjacent to the wound demonstrated the highest up-regulation of these molecules, they were generally reduced in migratory cells, much the same as our observation of reduced tenascin label in cells anterior to the compressed lamina cribrosa (Figure 7C and 7D). Vitronectin was also more heavily represented in the peripapillary sclera and lamina cribrosa of normal eyes, reflecting a similar affinity for tissues of high stress. In support of this, glaucoma specimens with significant damage demonstrated the heaviest label in the anterior portions of the compressed lamina cribrosa (Figure 7E and 7F).

This pattern of label is reminiscent of earlier observations that chondroitin sulfate PG are similarly localized to the load-bearing sclera and lamina cribrosa.³⁶ Specific evaluations of aggrecan, a high-molecular-weight chondroitin sulfate containing PG, further supports this finding (Figure 15).

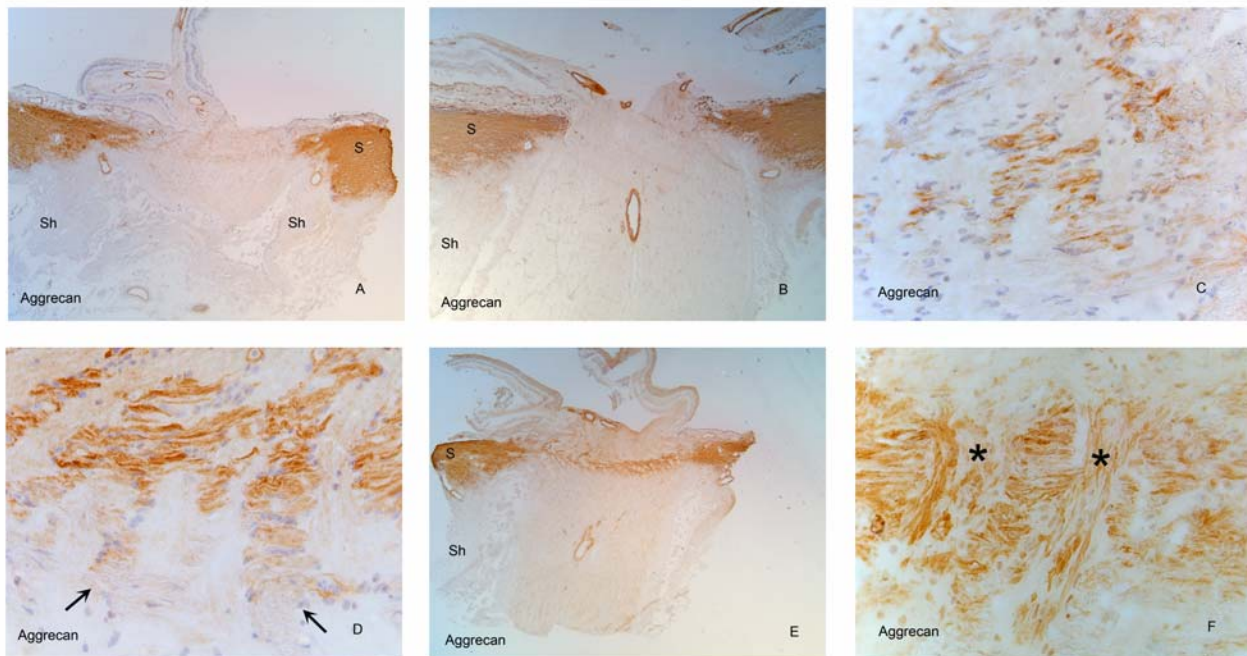


FIGURE 15

Aggrecan label in normal and glaucomatous eyes. Antibodies to the large chondroitin sulfate proteoglycan aggrecan selectively labels tissues subjected to high stress (A and B), including the sclera and blood vessel walls, but not tissues that experience lower stress, such as the optic nerve sheath (Sh) and the pia mater. Lamina cribrosa demonstrates variable results, with light label (C) of laminar beams in some specimens (same eye as A), and more intense labeling in others (D), with reduced intensity over the more posterior beams (arrows). Eyes with moderate optic nerve damage from primary open-angle glaucoma typically demonstrate heavier label of lamina (E and F), with abnormal deposits (*) between laminar beams. (Magnification: A, $\times 17$; B, $\times 17$; C, $\times 272$; D, $\times 272$; E, $\times 17$; F, $\times 272$)

This PG, primarily seen in regions of high stress, such as cartilage, provides a cushioning effect for these tissues and may serve a similar function in the posterior sclera. In fact, cyclic strain in chondrocytes has been shown to stimulate production of aggrecan and increase expression for $\alpha 2$ and $\alpha 5$ integrin subunits.⁹³ Whereas the greatest label with aggrecan antibodies was seen in the glaucoma specimens, label to the lamina cribrosa in normal eyes was somewhat variable. Many normal eyes demonstrated only minimal label of the lamina cribrosa, but label was easily detected in others. Interestingly, in these eyes, the distribution showed a more intense label over the anterior portions of the lamina, and much less label over the more posterior, heavily collagenous laminar beams (Figure 15C). This also suggests that the greater stresses in the normal optic nerve head may exist within the anterior laminar region.

It is noteworthy that the label of many integrin subtypes in the current study also appear to be most dense just anterior to the lamina cribrosa. This likely reflects the very high concentration of astrocytes in this region (Figure 5). In addition, several of these antibodies demonstrate an increased overall stain in this region, even within the axon bundles, suggesting that there may be some label of not only the cell bodies, but the astrocyte processes as well, as they enter the axon bundles and interdigitate with the axons to provide physical and nutritional support. This is supported by Figure 16, which shows label of a nonhuman primate eye with antibodies to glial fibrillary acidic protein (GFAP), the main intermediate filament protein of glial cells. This demonstrates a generally heavier label just anterior to the lamina, which on higher-power examination appears to be a remarkably dense network of cell processes throughout the optic nerve head. The orientation of these fibers just anterior to the lamina is primarily transverse and suggests that these cells are ideally situated to sense transverse stresses, as might be seen with elevations and fluctuation of IOP.

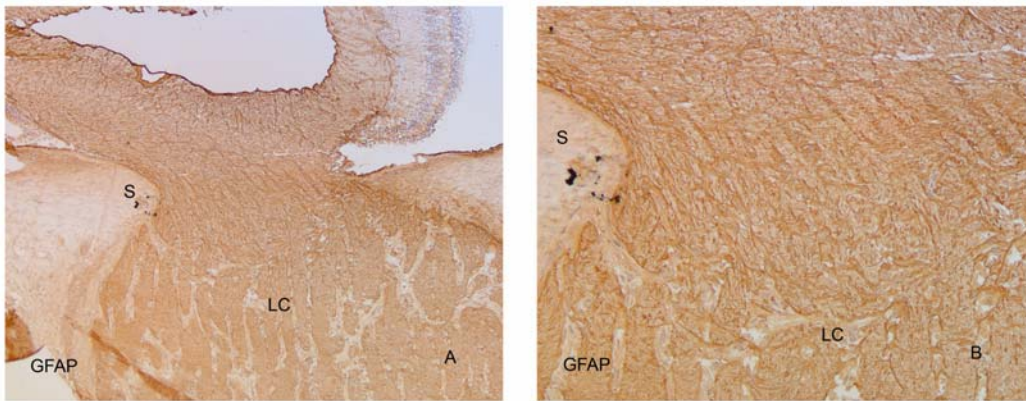


FIGURE 16

Nonhuman primate optic nerve head labeled with antibodies to GFAP. Note increased density of label (A) just anterior to the lamina cribrosa (LC). On higher power (B) this appears to be related to astrocytes of the glial columns and their transverse processes. (Magnification: A, $\times 17$; B, $\times 136$)

CONCLUSION

This systematic study of integrin subunits has demonstrated that these molecules have a substantial presence in the normal optic nerve head. When matched with their known ligands and the distribution of the ECM within the optic nerve head, these appear to be primarily associated with astrocytes and vascular cells, along with a suggestion that some may be associated with microglia as well. Considering that integrins provide attachments between connective tissues and the cytoskeleton, and the wide range of cellular responses that they mediate, integrins appear to be ideal candidates for translating physical stress and strain into the cellular responses known to occur in glaucomatous optic neuropathy.

The association of many of these integrin subunits with astrocytes lining the beams of the lamina cribrosa supports the concept that these cells participate actively in these responses. The heavy label with many of these antibodies anterior to the lamina cribrosa in glaucomatous tissues, and distinctly altered label with others, suggests that stress and strain anterior to the lamina may play a particularly important role.

ACKNOWLEDGMENTS

The author wishes to acknowledge the help of Elaine Johnson, ScD, who contributed to grading and interpretation of the immunohistochemistry results and reviewed this manuscript. William Cepurna, BS, provided valuable assistance with preparation and printing of the illustrations. Kristen Steele, BA, Susan Farrell, BA, Lisa Deppmeier, BS, and Stacy Barbur, BS, contributed to immunohistochemistry of these tissues.

The author was responsible for obtaining and interpreting clinical data on the glaucomatous eyes. He personally examined and graded the labeling intensity and distribution of these antibodies in all normal and glaucomatous tissues and performed all of the photomicroscopic documentation of these findings. Interpretation of findings in normal tissues, comparisons between normal and

glaucomatous tissues and correlations with the literature, and their contribution to the biomechanical theory of glaucomatous optic neuropathy were all performed by the author, as was the writing of this thesis.

REFERENCES

1. Friedman DS, Wolfs RC, O'Colmain BJ, et al. Prevalence of open-angle glaucoma among adults in the United States. *Arch Ophthalmol* 2004;122:532-538.
2. Quigley HA. New paradigms in the mechanisms and management of glaucoma. *Eye* 2005;19:1241-1248.
3. Tielsch JM, Sommer A, Katz J, et al. Racial variations in the prevalence of primary open-angle glaucoma. The Baltimore Eye Survey. *JAMA* 1991;266:369-374.
4. Mitchell P, Smith W, Attebo K, et al. Prevalence of open-angle glaucoma in Australia. The Blue Mountains Eye Study. *Ophthalmology* 1996;103:1661-1669.
5. Klein BE, Klein R, Sponsel WE, et al. Prevalence of glaucoma. The Beaver Dam Eye Study. *Ophthalmology* 1992;99:1499-1504.
6. Sommer A. Intraocular pressure and glaucoma. *Am J Ophthalmol* 1989;107:186-188.
7. AGIS-Investigators. The Advanced Glaucoma Intervention Study (AGIS): 7. The relationship between control of intraocular pressure and visual field deterioration. *Am J Ophthalmol* 2000;130:429-440.
8. Schulzer M, Alward WL, Feldman F, et al. Comparison of glaucomatous progression between untreated patients with normal-tension glaucoma and patients with therapeutically reduced intraocular pressures. *Am J Ophthalmol* 1998;126:487-497.
9. Kass MA, Heuer DK, Higginbotham EJ, et al. The Ocular Hypertension Treatment Study: a randomized trial determines that topical ocular hypotensive medication delays or prevents the onset of primary open-angle glaucoma. *Arch Ophthalmol* 2002;120:701-713.
10. Bellezza AJ, Hart RT, Burgoyne CF. The optic nerve head as a biomechanical structure: initial finite element modeling. *Invest Ophthalmol Vis Sci* 2000;41:2991-3000.
11. Burgoyne CF, Downs JC, Bellezza AJ, et al. The optic nerve head as a biomechanical structure: a new paradigm for understanding the role of IOP-related stress and strain in the pathophysiology of glaucomatous optic nerve head damage. *Prog Retin Eye Res* 2005;24:39-73.
12. Burgoyne CF, Downs JC, Bellezza AJ, et al. Three-dimensional reconstruction of normal and early glaucoma monkey optic nerve head connective tissues. *Invest Ophthalmol Vis Sci* 2004;45:4388-4399.
13. Geiger B, Bershadsky A. Exploring the neighborhood: adhesion-coupled cell mechanosensors. *Cell* 2002;110:139-142.
14. Geiger B, Bershadsky A. Assembly and mechanosensory function of focal contacts. *Curr Opin Cell Biol* 2001;13:584-592.
15. Hynes RO. Integrins: bidirectional, allosteric signaling machines. *Cell* 2002;110:673-687.
16. Quigley HA, Addicks EM, Green WR, et al. Optic nerve damage in human glaucoma. II. The site of injury and susceptibility to damage. *Arch Ophthalmol* 1981;99:635-649.
17. Quigley HA, Hohman RM, Addicks EM, et al. Morphologic changes in the lamina cribrosa correlated with neural loss in open-angle glaucoma. *Am J Ophthalmol* 1983;95:673-691.
18. Quigley HA, Green WR. The histology of human glaucoma cupping and optic nerve damage: clinicopathologic correlation in 21 eyes. *Ophthalmology* 1979;86:1803-1830.
19. Sommer A, Katz J, Quigley HA, et al. Clinically detectable nerve fiber atrophy precedes the onset of glaucomatous field loss. *Arch Ophthalmol* 1991;109:77-83.
20. Tuulonen A, Airaksinen PJ. Initial glaucomatous optic disk and retinal nerve fiber layer abnormalities and their progression. *Am J Ophthalmol* 1991;111:485-490.
21. Quigley HA, Addicks EM. Regional differences in the structure of the lamina cribrosa and their relation to glaucomatous optic nerve damage. *Arch Ophthalmol* 1981;99:137-143.
22. Anderson DR. Ultrastructure of human and monkey lamina cribrosa and optic nerve head. *Arch Ophthalmol* 1969;82:800-814.
23. Anderson DR. Ultrastructure of the optic nerve head. *Arch Ophthalmol* 1970;83:63-73.
24. Hayreh SS. Blood supply of the optic nerve head and its role in optic atrophy, glaucoma, and oedema of the optic disc. *Br J Ophthalmol* 1969;53:721-748.
25. Morrison JC, DeFrank MP, Van Buskirk EM. Comparative microvascular anatomy of mammalian ciliary processes. *Invest Ophthalmol Vis Sci* 1987;28:1325-1340.
26. Morrison JC, Van Buskirk EM. Sequential microdissection and scanning electron microscopy of ciliary microvascular castings. *Scan Electron Microsc* 1984;(Pt 2):857-865.
27. Cioffi GA, Van Buskirk EM. Microvasculature of the anterior optic nerve. *Surv Ophthalmol* 1994;38 Suppl:S107-116; discussion S116-107.
28. Hernandez MR, Igoe F, Neufeld AH. Extracellular matrix of the human optic nerve head. *Am J Ophthalmol* 1986;102:139-148.
29. Hernandez MR, Luo XX, Igoe F, et al. Extracellular matrix of the human lamina cribrosa. *Am J Ophthalmol* 1987;104:567-576.
30. Hernandez MR, Luo XX, Andrzejewska W, et al. Age-related changes in the extracellular matrix of the human optic nerve head. *Am J Ophthalmol* 1989;107:476-484.
31. Morrison JC, Jerdan JA, L'Hernault NL, et al. The extracellular matrix composition of the monkey optic nerve head. *Invest Ophthalmol Vis Sci* 1988;29:1141-1150.

32. Morrison JC, Jerdan JA, Dorman ME, et al. Structural proteins of the neonatal and adult lamina cribrosa. *Arch Ophthalmol* 1989;107:1220-1224.
33. Morrison JC, L'Hernault NL, Jerdan JA, et al. Ultrastructural location of extracellular matrix components in the optic nerve head. *Arch Ophthalmol* 1989;107:123-129.
34. Morrison J, Farrell S, Johnson E, et al. Structure and composition of the rodent lamina cribrosa. *Exp Eye Res* 1995;60:127-135.
35. Morrison JC, Johnson EC, Cepurna WO, et al. Microvasculature of the rat optic nerve head. *Invest Ophthalmol Vis Sci* 1999;40:1702-1709.
36. Morrison JC, Rask P, Johnson EC, et al. Chondroitin sulfate proteoglycan distribution in the primate optic nerve head. *Invest Ophthalmol Vis Sci* 1994;35:838-845.
37. Minckler DS, Bunt AH, Johanson GW. Orthograde and retrograde axoplasmic transport during acute ocular hypertension in the monkey. *Invest Ophthalmol Vis Sci* 1977;16:426-441.
38. Minckler DS, Bunt AH, Klock IB. Radioautographic and cytochemical ultrastructural studies of axoplasmic transport in the monkey optic nerve head. *Invest Ophthalmol Vis Sci* 1978;17:33-50.
39. Quigley H, Anderson DR. The dynamics and location of axonal transport blockade by acute intraocular pressure elevation in primate optic nerve. *Invest Ophthalmol* 1976;15:606-616.
40. Quigley HA, Anderson DR. Distribution of axonal transport blockade by acute intraocular pressure elevation in the primate optic nerve head. *Invest Ophthalmol Vis Sci* 1977;16:640-644.
41. Quigley HA, Guy J, Anderson DR. Blockade of rapid axonal transport. Effect of intraocular pressure elevation in primate optic nerve. *Arch Ophthalmol* 1979;97:525-531.
42. Quigley HA, Addicks EM. Chronic experimental glaucoma in primates. II. Effect of extended intraocular pressure elevation on optic nerve head and axonal transport. *Invest Ophthalmol Vis Sci* 1980;19:137-152.
43. Quigley HA, McKinnon SJ, Zack DJ, et al. Retrograde axonal transport of BDNF in retinal ganglion cells is blocked by acute IOP elevation in rats. *Invest Ophthalmol Vis Sci* 2000;41:3460-3466.
44. Hernandez MR, Andrzejewska WM, Neufeld AH. Changes in the extracellular matrix of the human optic nerve head in primary open-angle glaucoma. *Am J Ophthalmol* 1990;109:180-188.
45. Morrison JC, Dorman-Pease ME, Dunkelberger GR, et al. Optic nerve head extracellular matrix in primary optic atrophy and experimental glaucoma. *Arch Ophthalmol* 1990;108:1020-1024.
46. Hernandez MR, Ye H, Roy S. Collagen type 4 gene expression in human optic nerve heads with primary open angle glaucoma. *Exp Eye Res* 1994;59:41-51.
47. Morrison JC, Moore CG, Deppmeier LM, et al. A rat model of chronic pressure-induced optic nerve damage. *Exp Eye Res* 1997;64:85-96.
48. Johnson EC, Morrison JC, Farrell S, et al. The effect of chronically elevated intraocular pressure on the rat optic nerve head extracellular matrix. *Exp Eye Res* 1996;62:663-674.
49. Johnson EC, Deppmeier LM, Wentzien SK, et al. Chronology of optic nerve head and retinal responses to elevated intraocular pressure. *Invest Ophthalmol Vis Sci* 2000;41:431-442.
50. Pena JD, Varela HJ, Ricard CS, et al. Enhanced tenascin expression associated with reactive astrocytes in human optic nerve heads with primary open angle glaucoma. *Exp Eye Res* 1999;68:29-40.
51. Agapova OA, Ricard CS, Salvador-Silva M, et al. Expression of matrix metalloproteinases and tissue inhibitors of metalloproteinases in human optic nerve head astrocytes. *Glia* 2001;33:205-216.
52. Agapova OA, Kaufman PL, Lucarelli MJ, et al. Differential expression of matrix metalloproteinases in monkey eyes with experimental glaucoma or optic nerve transection. *Brain Res* 2003;967:132-143.
53. Varela HJ, Hernandez MR. Astrocyte responses in human optic nerve head with primary open-angle glaucoma. *J Glaucoma* 1997;6:303-313.
54. Hernandez MR, Agapova OA, Yang P, et al. Differential gene expression in astrocytes from human normal and glaucomatous optic nerve head analyzed by cDNA microarray. *Glia* 2002;38:45-64.
55. Yang P, Agapova O, Parker A, et al. DNA microarray analysis of gene expression in human optic nerve head astrocytes in response to hydrostatic pressure. *Physiol Genomics* 2004;17:157-169.
56. Flammer J, Orgul S. Optic nerve blood-flow abnormalities in glaucoma. *Prog Retin Eye Res* 1998;17:267-289.
57. Geijer C, Bill A. Effects of raised intraocular pressure on retinal, prelaminar, laminar, and retrolaminar optic nerve blood flow in monkeys. *Invest Ophthalmol Vis Sci* 1979;18:1030-1042.
58. van der Flier A, Sonnenberg A. Function and interactions of integrins. *Cell Tissue Res* 2001;305:285-298.
59. Plow EF, Haas TA, Zhang L, et al. Ligand binding to integrins. *J Biol Chem* 2000;275:21785-21788.
60. Humphries MJ. Integrin structure. *Biochem Soc Trans* 2000;28:311-339.
61. Liddington RC, Ginsberg MH. Integrin activation takes shape. *J Cell Biol* 2002;158:833-839.
62. Rezniczek GA, de Pereda JM, Reipert S, et al. Linking integrin alpha6beta4-based cell adhesion to the intermediate filament cytoskeleton: direct interaction between the beta4 subunit and plectin at multiple molecular sites. *J Cell Biol* 1998;141:209-225.
63. Liu B, Neufeld AH. Activation of epidermal growth factor receptor causes astrocytes to form cribriform structures. *Glia* 2004;46:153-168.
64. Hernandez MR. The optic nerve head in glaucoma: role of astrocytes in tissue remodeling. *Prog Retin Eye Res* 2000;19:297-321.

65. Grooms SY, Terracio L, Jones LS. Anatomical localization of beta 1 integrin-like immunoreactivity in rat brain. *Exp Neurol* 1993;122:253-259.
66. Tawil NJ, Wilson P, Carbonetto S. Expression and distribution of functional integrins in rat CNS glia. *J Neurosci Res* 1994;39:436-447.
67. Paulus W, Baur I, Schuppan D, et al. Characterization of integrin receptors in normal and neoplastic human brain. *Am J Pathol* 1993;143:154-163.
68. Guidry C, Bradley KM, King JL. Tractional force generation by human muller cells: growth factor responsiveness and integrin receptor involvement. *Invest Ophthalmol Vis Sci* 2003;44:1355-1363.
69. de Curtis I, Reichardt LF. Function and spatial distribution in developing chick retina of the laminin receptor alpha 6 beta 1 and its isoforms. *Development* 1993;118:377-388.
70. Brem RB, Robbins SG, Wilson DJ, et al. Immunolocalization of integrins in the human retina. *Invest Ophthalmol Vis Sci* 1994;35:3466-3474.
71. Davies PF, Robotewskyj A, Griem ML. Quantitative studies of endothelial cell adhesion. Directional remodeling of focal adhesion sites in response to flow forces. *J Clin Invest* 1994;93:2031-2038.
72. Bader BL, Rayburn H, Crowley D, et al. Extensive vasculogenesis, angiogenesis, and organogenesis precede lethality in mice lacking all alpha v integrins. *Cell* 1998;95:507-519.
73. Robbins SG, Brem RB, Wilson DJ, et al. Immunolocalization of integrins in proliferative retinal membranes. *Invest Ophthalmol Vis Sci* 1994;35:3475-3485.
74. Fukuchi T, Ueda J, Abe H, et al. Cell adhesion glycoproteins in the human lamina cribrosa. *Jpn J Ophthalmol* 2001;45:363-367.
75. Wagner S, Tagaya M, Koziol JA, et al. Rapid disruption of an astrocyte interaction with the extracellular matrix mediated by integrin alpha 6 beta 4 during focal cerebral ischemia/reperfusion. *Stroke* 1997;28:858-865.
76. Neufeld AH. Microglia in the optic nerve head and the region of parapapillary chorioretinal atrophy in glaucoma. *Arch Ophthalmol* 1999;117:1050-1056.
77. Kloss CU, Bohatschek M, Kreutzberg GW, et al. Effect of lipopolysaccharide on the morphology and integrin immunoreactivity of ramified microglia in the mouse brain and in cell culture. *Exp Neurol* 2001;168:32-46.
78. Milner R, Campbell IL. The extracellular matrix and cytokines regulate microglial integrin expression and activation. *J Immunol* 2003;170:3850-3858.
79. Nasu-Tada K, Koizumi S, Inoue K. Involvement of beta1 integrin in microglial chemotaxis and proliferation on fibronectin: different regulations by ADP through PKA. *Glia* 2005;52:98-107.
80. Tagaya M, Haring HP, Stuiiver I, et al. Rapid loss of microvascular integrin expression during focal brain ischemia reflects neuron injury. *J Cereb Blood Flow Metab* 2001;21:835-846.
81. Webb DJ, Parsons JT, Horwitz AF. Adhesion assembly, disassembly and turnover in migrating cells—over and over and over again. *Nat Cell Biol* 2002;4:E97-100.
82. Juliano RL, Reddig P, Alahari S, et al. Integrin regulation of cell signalling and motility. *Biochem Soc Trans* 2004;32:443-446.
83. Brooks PC, Stromblad S, Sanders LC, et al. Localization of matrix metalloproteinase MMP-2 to the surface of invasive cells by interaction with integrin alpha v beta 3. *Cell* 1996;85:683-693.
84. Bill HM, Knudsen B, Moores SL, et al. Epidermal growth factor receptor-dependent regulation of integrin-mediated signaling and cell cycle entry in epithelial cells. *Mol Cell Biol* 2004;24:8586-8599.
85. Cambier S, Gline S, Mu D, et al. Integrin alpha(v)beta8-mediated activation of transforming growth factor-beta by perivascular astrocytes: an angiogenic control switch. *Am J Pathol* 2005;166:1883-1894.
86. Hynes RO, Lively JC, McCarty JH, et al. The diverse roles of integrins and their ligands in angiogenesis. *Cold Spring Harb Symp Quant Biol* 2002;67:143-153.
87. McCarty JH, Monahan-Earley RA, Brown LF, et al. Defective associations between blood vessels and brain parenchyma lead to cerebral hemorrhage in mice lacking alphav integrins. *Mol Cell Biol* 2002;22:7667-7677.
88. Friedlander M, Theesfeld CL, Sugita M, et al. Involvement of integrins alpha v beta 3 and alpha v beta 5 in ocular neovascular diseases. *Proc Natl Acad Sci U S A* 1996;93:9764-9769.
89. Mackie EJ. Tenascin in connective tissue development and pathogenesis. *Perspect Dev Neurobiol* 1994;2:125-132.
90. Chiquet-Ehrismann R, Chiquet M. Tenascins: regulation and putative functions during pathological stress. *J Pathol* 2003;200:488-499.
91. Chiquet M, Sarasa-Renedo A, Tunc-Civelek V. Induction of tenascin-C by cyclic tensile strain versus growth factors: distinct contributions by Rho/ROCK and MAPK signaling pathways. *Biochim Biophys Acta* 2004;1693:193-204.
92. Nishio T, Kawaguchi S, Yamamoto M, et al. Tenascin-C regulates proliferation and migration of cultured astrocytes in a scratch wound assay. *Neuroscience* 2005;132:87-102.
93. Lahiji K, Polotsky A, Hungerford DS, et al. Cyclic strain stimulates proliferative capacity, alpha2 and alpha5 integrin, gene marker expression by human articular chondrocytes propagated on flexible silicone membranes. *In Vitro Cell Dev Biol Anim* 2004;40:138-142.